LBL-25956
Preprint

# Lawrence Berkeley Laboratory
UNIVERSITY OF CALIFORNIA

RECEIVED
LAWRENCE
BERKELEY LABORATORY

APR 17 1989

LIBRARY AND
DOCUMENTS SECTION

To be submitted for publication

## Hadron to Quark-Gluon Phase Transition in the Baryon Rich Domain

N.K. Glendenning

January 1989

TWO-WEEK LOAN COPY

This is a Library Circulating Copy
which may be borrowed for two weeks.

NUCLEAR SCIENCE DIVISION

LBL-25956 c.2

Prepared for the U.S. Department of Energy under Contract Number DE-AC03-76SF00098.

## DISCLAIMER

This document was prepared as an account of work sponsored by the United States Government. While this document is believed to contain correct information, neither the United States Government nor any agency thereof, nor the Regents of the University of California, nor any of their employees, makes any warranty, express or implied, or assumes any legal responsibility for the accuracy, completeness, or usefulness of any information, apparatus, product, or process disclosed, or represents that its use would not infringe privately owned rights. Reference herein to any specific commercial product, process, or service by its trade name, trademark, manufacturer, or otherwise, does not necessarily constitute or imply its endorsement, recommendation, or favoring by the United States Government or any agency thereof, or the Regents of the University of California. The views and opinions of authors expressed herein do not necessarily state or reflect those of the United States Government or any agency thereof or the Regents of the University of California.

LBL-25956

# Hadron to Quark-Gluon Phase Transition in the Baryon Rich Domain†

Norman K. Glendenning

*Nuclear Science Division*
*Lawrence Berkeley Laboratory*
*1 Cyclotron Road*
*Berkeley, CA 94720*

January 17, 1989

†This work was supported by the Director, Office of Energy Research, Office of High Energy and Nuclear Physics, Division of Nuclear Physics, of the U.S. Department of Energy under Contract DE-AC03-76SF00098.

# Hadron to Quark-Gluon Phase Transition in the Baryon Rich Domain†

Norman K. Glendenning

*Nuclear Science Division*
*Lawrence Berkeley Laboratory*
*1 Cyclotron Road*
*Berkeley, CA 94720*

January 17, 1989

**Abstract**

The hadron to quark-gluon phase transition is studied in charge symmetric matter. Nuclear field theory describes the hadronic phase, including baryon resonances and thermal pions and kaons. The pion dispersion in medium is computed. The other phase is described as a gas of massless $u$ and $d$ quarks and gluons and massive $s$ quarks, with or without gluon exchange. The Rankine-Hugoniot relation is employed to estimate the initial properties of matter produced in nuclear collisions as a function of energy. It is found that signals depending on pressure or entropy are poor ones and that the most dramatic differences between the hadronic phase and mixed phase occur in the temperature and density. Di-lepton and photon signals ought therefore to be good ones. It is shown that the analogy of "melting" of hadrons in the plasma is incorrect as concerns formation of a plasma in nuclear collisions in contrast to the adiabatic heating of matter. Neither the phase diagram nor the properties of matter on the shock trajectory depend very much on the nuclear equation of state within the uncertainties with which it can be defined in terms of conventional nuclear saturation properties, because the thermal energy dominates over these. The main dependances are on the hadron spectrum, the pion dispersion in medium, the bag constant and the QCD coupling constant. Within accepted uncertainties in the nuclear and plasma equations of state, the mixed phase could be formed in collisions with laboratory kinetic energy as low as 2.5 GeV.

**PACS 21.65+f, 25.70.Np, 0570.Fh**

†This work was supported by the Director, Office of Energy Research, Office of High Energy and Nuclear Physics, Division of Nuclear Physics, of the U.S. Department of Energy under Contract DE-AC03-76SF00098.

# Contents

**1 Introduction** **1**

**2 Hadronic Matter** **3**
2.1 Interacting Hadron Equation of State . . . . . 3
2.2 Coupling Constants and Equation of State . . . . . 6
2.3 Pion Spectrum in Nuclear Matter . . . . . 8

**3 Quark-Gluon Matter** **11**

**4 Results** **13**
4.1 Interpretation . . . . . 13
4.2 Approximation to Dynamics . . . . . 14
4.3 Phase Transition Dependance on Hadron Spectrum . . . . . 14
4.4 Properties on the Shock Trajectory . . . . . 15
4.5 Dependance on Bag Pressure . . . . . 17
4.6 Dependance on Gluon Exchange . . . . . 17
4.7 Dependance on Nuclear Compression $K$ . . . . . 18
4.8 Dependance on Pion Spectrum in Medium . . . . . 18

**5 Summary** **18**

# Hadron to Quark-Gluon Phase Transition in the Baryon Rich Domain

Norman K. Glendenning

January 17, 1989

## 1 Introduction

The most reliable predictions concerning the phase transition between hadronic matter and quark-gluon plasma are those of lattice gauge theory, which is a numerical solution of QCD [1,2]. Unfortunately, these predictions, for the foreseeable future do not encompass the actual physical means of investigating the phase transition in the laboratory. The lattice gauge calculations concern the adiabatic heating of uniform infinite matter. The experimental probe is a violent collision between nuclei. Indeed, up to the present, the lattice calculations pertain to a baryonless plasma, and are able to predict only one point in the phase diagram, the transition point at finite temperature but vanishing baryon density. The predicted transition temperature is $T \sim 200$ MeV. The lack of precision in the prediction arises from uncertainties in relating the scale parameter of the calculation to the physical scale because of the numerical difficulties still encountered in applying the theory to the confined states of single hadrons whose masses set the scale. But most important for the motivation of the present investigation is the gulf between the problem solved by lattice theory, and the nature of the experimental probe. The collision of nuclei, say a central one, at a given laboratory energy produces matter of some corresponding *definite* temperature and baryon density, *depending* on the collision dynamics. It will then evolve toward disassembly, possibly along an isentropic path. The entire phase diagram is therefore not accessible. The injection points will lie on a trajectory, each point of which corresponds to a given laboratory energy.

It is the purpose of this work, through models of the hadronic and quark gluon plasma phases, to investigate within reasonable parameterizations of each phase, the phase diagram, the trajectory in the phase diagram that is accessible in collisions of hadronic matter, and the properties of matter, and hence the possible signals, that correspond to the accessible region. Such a two model approach to studying

the phase transition has been investigated by a number of authors (see [3,4,5,6] and references therein). In this work we investigate a number of other features of this approach. On the hadronic side the well known bulk properties are the binding energy, saturation density and symmetry energy. In addition the effective nucleon mass at saturation is fairly established. There remains considerable debate over the compression modulus. On the quark side the principle uncertainty is the bag constant and the effect of interactions due to gluon exchange. Therefore $K$, $B$ and $\alpha_s$ will be the main focus as concerns uncertainties in the equation of state. We shall also investigate the role played by baryon resonances and shall include the pion polarization in the medium through the excitation of delta particle - nucleon hole excitations and the correlations introduced by the short range nuclear force. An interesting problem arises in connection with the appropriate weighting of the pion modes, which is discussed in detail.

Our investigation concerns the baryon rich plasma that is anticipated as a result of collisions at energies corresponding to the stopping of baryons within the volume of the colliding nuclei. In the energy domain where nuclear stopping is expected, there are two plausible means of estimating the temperature and density at which matter initially is made at given laboratory energy. One corresponds to the Rankine-Hugoniot shock condition, and the other to perfect stopping in the overlapping Lorentz contracted volume of the colliding nuclei. We shall compare these conditions. As well, we will calculate the accessible region of the phase diagram for several assumptions concerning the properties of hadronic matter, the nuclear equation of state, and for several assumptions concerning the quark-gluon phase, the bag pressure and the strong interaction coupling constant.

There is a region of the phase diagram that corresponds to a mixture of the two phases in equilibrium. There are commonly held assumptions concerning qualitative signals of the mixed phase. These are based on the observation that on an isotherm the pressure is constant as a function of energy throughout the mixed phase. While this is true, our first observation is that, unlike experiments on macroscopic systems, where the thermodynamic variables can be externally controlled, isotherms are not accessible in collisions. Our calculations of the trajectory of the injection point through the phase diagram that is probed as a function of laboratory energy correspond more closely to the actual nature of feasible experiments.

Relativistic nuclear field theory provides a good description of the bulk properties of nuclear matter as well as a large number of single-particle properties of finite nuclei [7]. With appropriate extensions, the theory can be used to study matter away from the normal state, matter that is under extreme conditions of temperature or density, such as is expected to be produced in relativistic nuclear collisions, and as formed in the collapse of a star just prior to the bounce that produces the supernova, and as exists in the cores of the neutron stars into which the remaining matter of the star subsides. We have studied some aspects of these problems in other papers, and refer to them for the formulation of the theory appropriate to the present application [8,9]. The new feature that we need here is the conservation

of strangeness, because the time scale of nuclear collisions is so short compared to the weak interaction scale that violates strangeness conservation. Strange baryons can be produced, but only in association with kaons, which do not decay during the collision, unlike the situation in neutron stars and supernova, where net strangeness can evolve, since it produces the lowest energy state of dense matter [10].

In addition to the scalar and vector mesons which mediate the baryon interactions at the mean field level, we take account of the contribution to the energy and pressure of other mesons, most notably the pion and kaon through their thermal distributions. The interaction response of the pion to the medium is taken into account through its coupling to delta-particle, nucleon-hole excitations and their repeated scatterings, which is believed to be the dominant contribution to the pion dispersion. Charged pions and kaons contribute to the electric charge, and kaons to the strangeness, which has to be taken into account in the constraints that must be imposed to describe non-strange charge-symmetric matter, as is appropriate for high energy nuclear collision.

We describe the quark gluon phase as a gas of massless up and down quarks and gluons and massive strange quarks. Again we are careful to conserve strangeness and electric charge.

In the following sections, we describe first our calculation of the equation of state of matter in the hadronic phase, including the pion spectrum in the medium. The equation of state of the quark-gluon plasma is briefly discussed. Then we show and discuss the results of the investigation of the various aspects of the problem mentioned above.

# 2 Hadronic Matter

## 2.1 Interacting Hadron Equation of State

The extended Lagrangian is [8,9]

$$\begin{aligned}\mathcal{L} &= \sum_B \overline{\psi}_B \Big[ i\gamma_\mu(\partial^\mu + i g_{\omega B}\omega^\mu) - (m_B - g_{\sigma B}\sigma)\Big]\psi_B \\ &\quad - \tfrac{1}{3} b m_n (g_\sigma \sigma)^3 - \tfrac{1}{4} c (g_\sigma \sigma)^4 + \tfrac{1}{2}(\partial_\mu \sigma \partial^\mu \sigma - m_\sigma^2 \sigma^2) \\ &\quad - \tfrac{1}{4}\omega_{\mu\nu}\omega^{\mu\nu} + \tfrac{1}{2} m_\omega^2 \omega_\mu \omega^\mu + \cdots \end{aligned} \tag{1}$$

Here $\psi_B$ denotes a baryon spinor and the sum is over *all the charge states* of the baryon families, N, $\Delta, \Lambda, \Sigma, \Xi$ as listed in table 1. The unstable baryon resonances are not included because the interactions through the meson exchange are explicitly incorporated [11]. The $\sigma$- and $\omega$-mesons are Yukawa coupled to the baryon scalar density and vector current, and the $\rho$-meson is coupled to the total isospin current which however vanishes in symmetric matter. The other mesons are included as free thermal bosons and their Lagrangians are represented by the ellipsis. We include the pion dispersion in the medium due to $N^{-1}\Delta$ excitations in calculating the boson distribution function.

The field equations for static uniform matter in the mean field approximation are, for the mesons,

$$m_\sigma^2\sigma = -bm_n(g_\sigma\sigma)^2 - c(g_\sigma\sigma)^3 + \sum_B g_{\sigma B} < \bar{\psi}\psi > \tag{2}$$

$$m_\omega^2\omega_0 = \sum_B g_{\omega B} < \psi^\dagger\psi > \tag{3}$$

$$m_\omega^2\omega_k = \sum_B g_{\omega B} < \bar{\psi}\gamma_k\psi > = 0 \implies \omega_k \equiv 0 \tag{4}$$

and for the baryons,

$$\Big[\gamma^\mu(p_\mu - g_{\omega B}\omega_\mu) - (m_B - g_{\sigma B}\sigma)\Big]\psi_B = 0. \tag{5}$$

The baryon eigenvalues of momentum, $k$, for particle and antiparticle are,

$$\epsilon_B(k) = E_B(k) + g_{\omega B}\omega_0 \tag{6}$$

$$\bar{\epsilon}_B(k) = E_B(k) - g_{\omega B}\omega_0, \tag{7}$$

with

$$E_B(k) = \sqrt{k^2 + (m_B - g_{\sigma B}\sigma)^2}. \tag{8}$$

For the present application we need the finite temperature solutions. The formulation has been carried out earlier [8,9]. Since the time scale (unlike supernovae or neutron stars) is very short on the weak interaction time ($\tau \sim 10^{-10}$ sec), strangeness is conserved throughout the duration of the collision and the evolution of its products. This does not mean that hyperons and kaons cannot occur in the hot dense matter that is formed, but only that the net strangeness is zero. Similarly, the total electric charge and the baryon number are conserved. For symmetric nuclear matter the charge density is $q = \rho/2$. These conservation laws can be enforced in the usual way, through the introduction of chemical potentials, $\mu_b, \mu_q$ and $\mu_s$, for (positive) baryon number, electric charge and strangeness, respectively. They together with the field amplitudes $\sigma, \omega_0$, can be determined through the three equations expressing the conservation laws and the two field equations. They are,

$$\rho = \sum_B \frac{2J_B+1}{2\pi^2} b_B \int_0^\infty (\exp[(\epsilon_B(k)-\mu_B)/T]+1)^{-1}\, k^2dk \tag{9}$$

$$\frac{\rho}{2} = \sum_B \frac{2J_B+1}{2\pi^2} q_B \int_0^\infty (\exp[(\epsilon_B(k)-\mu_B)/T]+1)^{-1}\, k^2dk + \sum_M \frac{2J_M+1}{2\pi^2} q_M \int_0^\infty (\exp[(\omega_M(k)-\mu_M)/T]-1)^{-1}\, k^2dk \tag{10}$$

$$0 = \sum_B \frac{2J_B+1}{2\pi^2} s_B \int_0^\infty (\exp[(\epsilon_B(k)-\mu_B)/T]+1)^{-1}\, k^2dk + \sum_M \frac{2J_M+1}{2\pi^2} s_M \int_0^\infty (\exp[(\omega_M(k)-\mu_M)/T]-1)^{-1}\, k^2dk \tag{11}$$

$$
\begin{aligned}
m_\sigma^2\sigma &= -bm_n(g_\sigma\sigma)^2 - c(g_\sigma\sigma)^3 \\
&\quad + \sum_B \frac{2J_B+1}{2\pi^2} g_{\sigma B} \\
&\quad \times \int_0^\infty \frac{m_B - g_{\sigma B}\sigma}{\sqrt{k^2+(m_B-g_{\sigma B}\sigma)^2}} (\exp[(\epsilon_B(k)-\mu_B)/T]+1)^{-1}\ k^2dk \qquad (12)
\end{aligned}
$$

$$
m_\omega^2\omega_0 = \sum_B \frac{2J_B+1}{2\pi^2} g_{\omega B} b_B \int_0^\infty (\exp[(\epsilon_B(k)-\mu_B)/T]+1)^{-1}\ k^2dk \qquad (13)
$$

The sums $B$ and $M$ run over all charge states of particles *and* antiparticles of the species listed in table 1. The chemical potential for a hadron species with baryon charge, $b_i$, electric charge, $q_i$, and strangeness quantum number, $s_i$, is

$$
\mu_i = b_i\mu_b + q_i\mu_q + s_i\mu_s \qquad (14)
$$

The antiparticle chemical potentials are the negative of these.

The hadronic equation of state is,

$$
\begin{aligned}
p &= -\tfrac{1}{3}bm_n(g_\sigma\sigma)^3 - \tfrac{1}{4}c(g_\sigma\sigma)^4 - \tfrac{1}{2}m_\sigma^2\sigma^2 + \tfrac{1}{2}m_\omega^2\omega_0^2 \\
&\quad + \frac{1}{3}\sum_B \frac{2J_B+1}{2\pi^2} \\
&\quad \times \int_0^\infty \frac{k^2}{\sqrt{k^2+(m_B-g_{\sigma B}\sigma)^2}} (\exp[(\epsilon_B(k)-\mu_B)/T]+1)^{-1}\ k^2dk \\
&\quad + \frac{1}{3}\sum_M \frac{2J_M+1}{2\pi^2} \int_0^\infty \frac{k^2}{\omega_M(k)} (\exp[(\omega_M(k)-\mu_M)/T]-1)^{-1}\ k^2dk \qquad (15)
\end{aligned}
$$

$$
\begin{aligned}
\epsilon &= \tfrac{1}{3}bm_n(g_\sigma\sigma)^3 + \tfrac{1}{4}c(g_\sigma\sigma)^4 + \tfrac{1}{2}m_\sigma^2\sigma^2 + \tfrac{1}{2}m_\omega^2\omega_0^2 \\
&\quad + \sum_B \frac{2J_B+1}{2\pi^2} \\
&\quad \times \int_0^\infty \sqrt{k^2+(m_B-g_{\sigma B}\sigma)^2}\, (\exp[(\epsilon_B(k)-\mu_B)/T]+1)^{-1}\ k^2dkdp \\
&\quad + \sum_M \frac{2J_M+1}{2\pi^2} \int_0^\infty \omega_M(k)(\exp[(\omega_M(k)-\mu_M)/T]-1)^{-1}\ k^2dk \qquad (16)
\end{aligned}
$$

In these equations, $\sigma$ and $\omega_0$ denote the mean values of the scalar meson, and the time-like component of the $\omega$-meson. The space-like components vanish in isotropic matter. The net baryon density, is denoted by $\rho$. The energy for free mesons is $\omega_M(k) = \sqrt{m_M^2+k^2}$. (We write an explicit expression for the pressure because $p = -(\partial E/\partial V)_S$ does not provide a convenient calculational scheme since $T$ appears

as an extensive variable in $\epsilon = E/V$ written above and the entropy varies along an isotherm.)

The entropy density is also an important quantity,

$$s = \frac{p+\epsilon}{T} - \frac{1}{T}\sum_i \mu_i(\rho_i - \bar{\rho}_i) \tag{17}$$

where the sum, $i$, is over the various baryon and meson species and their charge states. ( The particles states of the kaon are $K^+$ and $K^0$ and the antiparticle states are $K^-$ and $\bar{K}^0$.) The conservation laws for charge and strangeness, ($q = \rho/2$, $S = 0$), can be used to simplify the sum in the last term, which is equal to $\rho(\mu_b + \mu_q/2)$.

The most important thermal meson contributions to the above expressions for $p$ and $\epsilon$ are the pion and kaon. Because the kaon interacts weakly, we use the free kaon dispersion, $\omega_K(k) = \sqrt{m_K^2 + k^2}$. However the pion interacts strongly with the medium and its energy, $\omega(k)$, is strongly modified from the free dispersion, $\sqrt{m_\pi^2 + k^2}$, as discussed below.

In all of our calculations except for one that is discussed later for contrast, we include the baryon states of Table 1 which interact as in Eq.1 through the Yukawa coupling of scalar ($\sigma$) and vector ($\omega$) mesons, and as well include thermal pions and kaons.

Table 1: Hadron states. Spin is J, charge is q and strangeness is s.

| | m (MeV) | J | q | s |
|---|---|---|---|---|
| N | 939 | 1/2 | 0,1 | 0 |
| $\Delta$ | 1232 | 3/2 | -1,0,1,2 | 0 |
| $\Lambda$ | 1115 | 1/2 | 0 | -1 |
| $\Sigma$ | 1190 | 1/2 | -1,0,1 | -1 |
| $\Xi$ | 1315 | 1/2 | -1,0 | -2 |
| $\pi$ | 139 | 0 | -1,0,1 | 0 |
| K | 494 | 0 | 0,1 | 1 |

## 2.2 Coupling Constants and Equation of State

The four coupling constants in the theory, $g_\sigma/m_\sigma$, $g_\omega/m_\omega$, $b$, $c$, are chosen so that the theory possesses the bulk properties of uniform symmetric matter, binding B/A = 16 MeV, saturation density $\rho = 0.15$ fm$^{-3}$. The compression modulus has been the subject of considerable debate. A decade ago it appeared to have been established as $K = 220 \pm 20$ MeV. Recent evidence suggests a value $K \sim 300$ MeV [12,13]. Evidence from high energy nuclear collisions is still provisional but suggests as high or higher value [14]. On the other hand the nucleon (Landau) effective mass at

saturation is believed to lie within rather narrow bounds of about $m^\star_{Landau}/m \sim 0.83 - 0.85$ [15], implying a scalar effective mass at saturation of about $m^\star_{sat}/m \equiv (m_n - g_\sigma \sigma_{sat})/m \sim 0.78 - 0.8$. where we relate the two effective masses by,

$$m^\star_{Landau} = \left(\frac{k}{\partial\epsilon(k)/\partial k}\right)_{k_F} = (m^\star_{sat.}{}^2 + k_F^2)^{\frac{1}{2}} \tag{18}$$

Since the range of uncertainty in $m^\star$ is so small we take 0.8 in all of the calculations. Of course nuclear matter properties do not determine the hyperon couplings. For simplicity we have assumed universal coupling.

In Fig.1 we show the equation of state corresponding to several values of $m^\star$ at fixed $K$ and vice versa. In the domain of validity of the theory, namely up to a few times nuclear density and below the transition to the quark-gluon plasma, both effect the form of the equation of state. For very high density $m^\star$ is most important. The reason for this is that the vector repulsion dominates all other terms in the equation of state,[1] and for given binding energy and saturation density, the vector coupling constant is uniquely determined by $m^\star$ through,

$$\frac{\epsilon_0}{\rho_0} = \frac{B}{A} + m_n = \left(\frac{g_\omega}{m_\omega}\right)^2 \rho_0 + \sqrt{k_0^2 + m^{\star 2}_{sat.}} \tag{19}$$

where the Fermi momentum at saturation, $k_0$, is related to the density in the usual way, $\rho_0 = 2k_0^3/(3\pi^2)$. (The above relation follows from the saturation condition $\partial(\epsilon/\rho)/\partial k = 0$ evaluated at $k = k_0$ and the field equation for $\omega_0$.) However as we shall see later, the transition to the quark-gluon plasma occurs at density far below where this asymptotic behavior governs the equation of state, and the relevant range of densities is shown in the figures. Since $m^\star$ is known within such a narrow range as quoted above [15], the main uncertainty in the nuclear equation of state lies in the value of $K$.

Table 2: Coupling constants for several K and for B/A = 16 MeV, $\rho = 0.15$ fm$^{-3}$, $a_{sym} = 32.5$ MeV and $m^\star_{sat}/m = 0.8$.

| K MeV | $(g_\sigma/m_\sigma)^2$ (fm)$^2$ | $(g_\omega/m_\omega)^2$ (fm)$^2$ | $(g_\rho/m_\rho)^2$ (fm)$^2$ | b | c |
|---|---|---|---|---|---|
| 220 | 9.678 | 4.356 | 5.025 | 0.01164 | -0.004042 |
| 250 | 9.216 | 4.356 | 5.025 | 0.008209 | 0.007385 |
| 300 | 8.492 | 4.356 | 5.025 | 0.002084 | 0.02780 |
| 350 | 7.820 | 4.356 | 5.025 | -0.004618 | 0.05015 |

[1]In the Astrophys. J. article of ref. [10] a careful analysis is given at eq.(62-63) and the surrounding text.

The greatest influence of the baryon resonances occurs at finite temperature, especially high temperature, as shown in Fig.2. The form of the energy as a function of density shown there for finite temperature should not be mistaken as indicating a bound state. The pressure is everywhere positive on these isotherms despite the negative slope of the energy near the origin (recall the note following eq.16). The energy is finite at zero (net) baryon density because of thermal mesons and baryon pairs, which means that the energy per (net) baryon becomes large near the origin. The pion dispersion in matter is incorporated in these calculations as described in the next section.

## 2.3 Pion Spectrum in Nuclear Matter

The pion cannot exist in nuclear matter with the properties of the free pion because of its strong interaction with the medium as emphasized long ago by Migdal [16]. It exists in matter partly as itself and partly absorbed by a nucleon particle-hole or delta particle-nucleon hole excitation ($\Delta - N^{-1}$) with the pion's quantum numbers. The pion spectrum, $\omega(k)$ in nuclear matter is obtained as the poles of the pion propagator, $\mathcal{D}(k,\omega)$, in the medium, ie. as the solutions of

$$\mathcal{D}^{-1}(k,\omega) \equiv \omega(k)^2 - m_\pi^2 - k^2 - \Pi(k,\omega(k)) = 0 \tag{20}$$

where $\Pi(k,\omega(k))$ is the proper polarization and represents the square of the energy change caused by such processes mentioned. The relativistic expression for the polarization, which reduces in the non-relativistic limit to the Lindhart function describing particle-hole excitations, has been obtained earlier [17]. However here we choose the more phenomenological approach of Migdal [16]. We approximate it by the dominant contribution, the pion coupling to the $\Delta - N^{-1}$ excitations and their repeated scatterings in nuclear matter at density $\rho$, and include finite-size vertex cutoffs. The resonance polarization is the sum of two uncrossed and two crossed graphs containing a delta and a delta plus two pions in the intermediate state respectively. In symmetric nuclear matter the polarization for the $\pi^+, \pi^0, \pi^-$ are all equal. It is [16,18],

$$\Pi_{res} \approx \frac{8}{9}\Big(\frac{g_\Delta k}{m_\pi}\Big)^2 \rho \frac{\omega_\Delta(k)}{\omega^2 - \omega_\Delta^2(k)} \tag{21}$$

The approximation sign above indicates the usual approximations including cancelation of the fermion momenta in the energy denominators. We keep the momentum dependance of the $\Delta - N^{-1}$ (resonance) dispersion, $\omega_\Delta$, in its relativistic form,

$$\omega_\Delta(k) = \sqrt{m_\Delta^2 + k^2} - m_n \tag{22}$$

The baryon masses here should be the scalar effective masses in matter, but for sake of illustration in this section we take them to have their vacuum values.

The repeated nuclear scatterings among $\Delta - N^{-1}$ states by the short range nuclear force characterized by the the Landau parameter, $g'$, when summed, yield the proper polarization,

$$\Pi(k,\omega(k)) = \frac{\Lambda^2(k)\Pi_{res}(k,\omega)}{1 - g'(m_\pi/g_\Delta k)^2\Lambda^2(k)\Pi_{res}(k,\omega)} \tag{23}$$

We include, as in Pandharipande [19], a vertex cutoff $\Lambda(k)$,

$$\Lambda(k) = \exp -\Big(\frac{k}{7m_\pi}\Big)^2 \tag{24}$$

The p-wave coupling strength, $g_\Delta$, of pions and nucleons to isobars is related in the quark model to the p-wave pion-nucleon coupling, $f$, by $g_\Delta = (6\sqrt{2}/5)f$, where $f^2/(4\pi) \sim 0.08$ [18]. The spin-isospin anti-symmetric Landau parameter for coupling of delta particle-nucleon hole states is $g' \sim 0.7(g_\Delta/m_\pi)^2$ [20].

By defining

$$B(k,\rho) = \frac{8}{9}\Big(\frac{g_\Delta}{m_\pi}\Big)^2\omega_\Delta(k)\Lambda^2(k)\rho, \qquad \gamma = g'\Big(\frac{m_\pi}{g_\Delta}\Big)^2 \tag{25}$$

the inverse pion propagator can be written

$$\mathcal{D}^{-1}(k,\omega) = \frac{(\omega^2-\omega_\pi^2)[(\omega^2-\omega_\Delta^2)-\gamma B]-k^2B}{(\omega^2-\omega_\Delta^2)-\gamma B} \tag{26}$$

which shows that there are two (positive) solutions, if $k$ and $\rho$ are finite. Otherwise for identically vanishing density, or infinite $k$, for which in both cases $B \equiv 0$, only the free solution exists (in the second case because of the momentum cutoff). Let us refer to the two solutions as $\omega_1(k)$ and $\omega_2(k)$. They are,

$$\omega_{2,1}^2 = \frac{1}{2}\Big[\omega_\Delta^2 + \gamma B + \omega_\pi^2 \pm \sqrt{(\omega_\Delta^2+\gamma B-\omega_\pi^2)^2 + 4k^2B}\Big]. \tag{27}$$

Both have to be taken into account and we show how to do this below. For small $k$ they have the limiting values,

$$\lim_{k\to 0}\omega_1(k) = \omega_\pi(0) = m_\pi \tag{28}$$

$$\lim_{k\to 0}\omega_2(k) = \sqrt{\omega_\Delta^2(0)+\gamma B} = \sqrt{(m_\Delta^2-m_n^2)^2+\gamma B} \tag{29}$$

and for large $k$,

$$\lim_{k\to\infty}\omega_1(k) = \omega_\Delta(k) \tag{30}$$

$$\lim_{k\to\infty}\omega_2(k) = \omega_\pi(k) \tag{31}$$

So at small $k$, we see that $\omega_1$ is pion-like while for large $k$ it is $\Delta$-like, and conversely for $\omega_2$.

For various values of the nuclear density we show the pion dispersion, $\omega(k)$ in Fig.3. One solution (for fixed density $\rho$) lies below the envelope defined by the free dispersion, $\omega_\pi(k) = \sqrt{m_\pi^2 + k^2}$, and the resonance dispersion, $\omega_\Delta(k)$, and the other lies above, referred to earlier as $\omega_1(k)$ and $\omega_2(k)$ respectively. In the limit of small (but not identically zero) density, neither solution represents the free dispersion at all $k$, since

$$\lim_{\rho\to 0}\omega_1(k) = \begin{cases} \omega_\pi(k) & \text{if } k < k_0 \\ \omega_\Delta(k) & \text{if } k > k_0 \end{cases} \tag{32}$$

$$\lim_{\rho\to 0}\omega_2(k) = \begin{cases} \omega_\Delta(k) & \text{if } k < k_0 \\ \omega_\pi(k) & \text{if } k > k_0 \end{cases} \tag{33}$$

where $k_0$ denotes the value of $k$ at which the free and resonance dispersions cross. Associated with this switch in behavior near $k_0$ are the weights for the pion-like component in the excitations 1 and 2. These weights, $A_i(k,\rho)$, will be proportional to the residues of the propagator (see appendix to ref. [17]) and the proportionality must be such that the temperature distribution for the free spectrum is recovered at vanishing density $\rho$. The residues are given by $1/(\partial\mathcal{D}^{-1}(k,\omega)/\partial\omega_i)$, $i = 1,2$, and the proportionality factor can be found as $2\omega_i$. Thus the weight of the pion-like component in the mode $i$ is,

$$A_i(k,\rho) = \Big(\frac{2\omega}{\partial\mathcal{D}^{-1}(k,\omega)/\partial\omega}\Big)_{\omega=\omega_i} \tag{34}$$

We can obtain the explicit expression for the weights,

$$A_i(k,\rho) = 1 - \frac{k^2 B(k,\rho)}{[\omega_i^2(k) - \omega_\Delta^2(k) - \gamma B(k,\rho)]^2 + k^2 B(k,\rho)} \tag{35}$$

and the sum rule,

$$A_1 + A_2 = 1. \tag{36}$$

This is most easily proven by rewriting the numerator of the inverse propagator Eq.26 in terms of its zeros, thus,

$$\mathcal{D}^{-1}(k,\omega) = \frac{(\omega^2 - \omega_1^2)(\omega^2 - \omega_2^2)}{\omega^2 - \omega_\Delta^2 - \gamma B} \tag{37}$$

whence the sum rule can be directly calculated. The weight, $A_2(k,\rho)$, is shown in Fig. 4 for the same densities as in Fig. 3. For vanishing density the weight becomes a step function at $k_0$. For *all* densities however the weights interchange the dominant character of the mode near $k_0$, with the pion-like component residing mostly in $\omega_1$ for $k < k_0$ and in $\omega_2$ otherwise except in the vicinity of $k_0$, where the weights are both about one half. Therefore, it is incorrect, in principle, to take account only of the $\omega_1$ solution as representing the pion excitation in high temperature matter

which can excite large $k$, because even though it lies lower in energy and has a larger thermal weight, it has vanishingly small spectral weight $A_1(k,\rho)$ for the pion-like component when $k$ is large. The weights discussed here are essential for processes that involve the identification of the pion component like di-lepton production from $\pi^+\pi^-$ annihilation [21].

The proper polarization and the spectrum of excitations with the pion quantum number was calculated above for symmetric nuclear matter assuming only neutrons and protons in occupied thermal states and allowing for pion absorption to form a delta in the intermediate state. In matter at high temperature and density, other baryon states will also be occupied, and because of the increasing scalar field as a function of density or temperature (decreasing effective mass), antibaryon states will also be occupied. It is very difficult to calculate these medium effects on the pion. We shall make only gross estimates of their effect on the polarization. We will include only the delta particle -nucleon hole excitations and also the antidelta particle-antinucleon hole excitations, in the scheme above. In the present work the contribution of the other baryon resonances to the pion polarization will be neglected. We do take into account in the subsequent calculations the effective nucleon and delta masses, $m_B^\star = m_B - g_\sigma\sigma$, as appear in the resonance dispersion.

Condensation of negative pions will occur if $\mu_{\pi^-}$ attains the value of the minimum of $\omega_1(k)$ from below. However the symmetry energy favors $\rho_n \approx \rho_p$ implying that $\mu_n \approx \mu_p$, while from Eq. 14, $\mu_{\pi^-} = \mu_n - \mu_p \approx 0$. In symmetric nuclear matter this is true for the other charge states of the pion also. Hence in this model of the proper polarization with the coupling $\gamma = g'(m_\pi/g_\Delta)^2 = 0.7$, pions do not condense below a density $\rho > 3$ fm$^{-3}$, as can be seen in Fig.3. [2] This is far above the density expected for the quark-gluon phase transition. Otherwise, the pion energy in the medium is clearly strongly modified at higher $\rho$ from its free value, $\omega_\pi(k) = \sqrt{m_\pi^2 + k^2}$, and we can anticipate that there is a tendency to raise the energy at which the phase transition will occur because of the energy trapped in low frequency thermally excited pions.

# 3 Quark-Gluon Matter

We describe the quark-gluon phase by the asymptotically free equation of state corresponding to a thermal mixture of massless $u$ and $d$ quarks and gluons and massive strange quarks with $m_s = 150$ MeV. An equal mixture of $u$ and $d$ quarks automatically has an electric charge to baryon ratio of 1/2, and this is not changed with the addition of a strangeness conserving mixture of $s$ and $\bar{s}$ quarks. Each quark flavor contributes the following to the pressure, energy density, baryon density and

[2]The situation is quite different in neutron stars where charge neutrality (which is a consequence of the fact that the Coulomb force is much stronger than the weak gravitational force which binds the star) assures that $\mu_n > \mu_p$. In this case negative pion condensation is a real possibility.

entropy density:

$$p = \frac{1}{3}\frac{\gamma_f}{2\pi^2}\int_0^\infty \frac{k^2}{\epsilon_f(k)}\Big(n(k,\mu_f)+n(k,-\mu_f)\Big)k^2dk - B \tag{38}$$

$$\epsilon = \frac{\gamma_f}{2\pi^2}\int_0^\infty \epsilon_f(k)\Big(n(k,\mu_f)+n(k,-\mu_f)\Big)k^2dk + B \tag{39}$$

$$\rho = \frac{1}{3}\frac{\gamma_f}{2\pi^2}\int_0^\infty \Big(n(k,\mu_f)-n(k,-\mu_f)\Big)k^2dk \tag{40}$$

$$s = \frac{S}{V} = \Big(\frac{\partial p}{\partial T}\Big)_{V,\mu_f} \tag{41}$$

where $\epsilon_f(k) = \sqrt{m_f^2 + k^2}$ and

$$n(k,\mu_f) = (exp[(\epsilon_f(k) - \mu_f)/T + 1)^{-1} \tag{42}$$

is the Fermi distribution function. The bag pressure is denoted by $B$, and represents the positive energy shift per unit volume in the deconfined vacuum relative to the confined vacuum. The quark degeneracy for each flavor is $\gamma_f = 2_{spin} \times 3_{color}$. For massless quarks these have the explicit forms;

$$p = \frac{7}{60}\pi^2T^4 + \frac{1}{2}T^2\mu_f^2 + \frac{1}{4\pi^2}\mu_f^4 - B \tag{43}$$

$$\epsilon = 3p + 4B \tag{44}$$

$$\rho = \frac{1}{3}\Big(T^2\mu_f + \frac{\mu_f^3}{\pi^2}\Big) \tag{45}$$

$$s = \frac{7}{15}\pi^2T^3 + T\mu_f^2 \tag{46}$$

For the massless Bose gas of gluons of degeneracy $2(N_c^2 - 1)$, we similarly obtain the contributions;

$$p = \frac{8\pi^2}{45}T^4 \tag{47}$$

$$\epsilon = 3p \tag{48}$$

$$s = \frac{32\pi^2}{45}T^3 \tag{49}$$

For massless quarks and gluons, we thus have, for example,

$$p = \frac{8\pi^2}{45}T^4 + \sum_f\Big(\frac{7}{60}\pi^2T^4 + \frac{1}{2}T^2\mu_f^2 + \frac{1}{4\pi^2}\mu_f^4\Big) - B \tag{50}$$

The lowest order gluon interactions have been calculated [22,23,24], and result in the following modification,

$$\begin{aligned} p = {} & \frac{8\pi^2}{45}T^4\Big(1 - \frac{15\alpha_s}{4\pi}\Big) \\ & + \sum_f\Big(\frac{7}{60}\pi^2T^4\Big(1 - \frac{50\alpha_s}{21\pi}\Big) + \Big(\frac{1}{2}T^2\mu_f^2 + \frac{1}{4\pi^2}\mu_f^4\Big)\Big(1 - \frac{2\alpha_s}{\pi}\Big)\Big) - B \end{aligned} \tag{51}$$

and corresponding changes in $\epsilon$, $s = \partial p/\partial T$ and $\rho = \frac{1}{3}\sum_f \partial p/\partial \mu_f$. The coupling constant is denoted by $\alpha_s$.

For a charge symmetric quark gas ($q = \rho/2$) with vanishing strangeness content, we must set

$$\mu_u = \mu_d, \qquad \mu_s = 0 \tag{52}$$

(Many authors have employed a common chemical potential for all flavors and apply a *factor* $N_f$ to the quark contributions to the $\epsilon, p$ etc. This is incorrect for $N_f = 3$, since such matter is neither charge symmetric nor has it zero strangeness.)

# 4 Results

## 4.1 Interpretation

In a complete theory of matter, it is possible (in principle) to calculate the thermodynamic variables at all densities, including the mixed phase region in cases where a first order phase transition occurs. The pressure on an isotherm as a function of density is illustrated in Fig.5 for such a case, by the solid line. The solid line between the end points of the mixed phase, (M, M') is actually not the physical state of the system, although it represents a solution of the theory. As is well known the physical state will consist of an equal pressure mixture of the two phases of matter at M and M' (the dashed line). These points correspond to the Gibbs criteria, which are the equality of pressure, temperature and baryon chemical potential ($3\mu_u = 3\mu_d = \mu_b$) in the two phases. The pressure remains constant in the mixed phase, and the other properties such as the energy, entropy, etc at a particular density between M and M' are equal to the volume mixture of the values at the end points. It should be noted that the highest density at which matter in the hadronic phase exists is the density corresponding to the point M. Since a complete solution of QCD for baryon rich matter will not be available for the foreseeable future, such a detailed curve for the phase transition between hadron and quark-gluon phase cannot be calculated in the region MM' (and the one solid one drawn is schematic). Instead we have two incomplete theories, nuclear field theory for the hadron phase and the free quark-gluon model of the second phase. The first does not describe the transition to an asymptotically free assembly of quarks and gluons at high energy density, and the second does not become a description of a confined assembly of hadrons at low energy density. The line HMH' shows the pressure in the hadron model and the line Q'M'Q shows it for the quark model. The physical path in the mixed phase, MM' can of course be identified by the Gibbs criteria. *If* indeed a phase transition does occur, the superheated portion of the hadron curve, MH' has no meaning, and approximates the true but unknown superheated state only in the vicinity of M. A similar statement holds for the supercooled quark phase M'Q'. In the report that follows, we shall show the portions of the hadron phase corresponding to MH' to show the properties of matter *if* no phase transition can occur under the conditions

studied, in order to contrast them with the properties that would obtain if there is a phase transition.

The phase diagram is most easily constructed by searching for the intersections of isotherms in the two phases in the $p-\mu$ plane. The density, energy, etc can then be calculated at the end points of the two phases since they correspond to the $\mu$ of the mixed phase which is the intersection. The phase diagram in the $T-\rho$ plane is shown in Fig.6, with the hadron, mixed and quark-gluon phases indicated. This corresponds to the particular choice of $K = 300$ MeV, and $B^{1/4} = 250$ MeV, as for Fig.5. We show later how variations in these change the phase diagram. All the hadron states of Table 1 are included.

## 4.2 Approximation to Dynamics

As discussed in the introduction, it is not possible experimentally to trace the properties on isotherms when the only way of preparing the matter is a collision. The collision dynamics, for each laboratory energy, will determine the initial state of the system. We make two approximations to the dynamics, one by assuming planar hydrodynamics so that a shock zone is formed, and the properties of matter in the zone are then prescribed in terms of the equation of state by the Rankine-Hugoniot relation,

$$\left(\frac{\rho}{\rho_0}\right)^2 = \frac{\epsilon(p+\epsilon)}{\epsilon_0(p+\epsilon_0)}, \qquad \gamma = \frac{\epsilon/\rho}{\epsilon_0/\rho_0} \tag{53}$$

and the other by assuming that the colliding nuclei stop each other in their overlapping Lorentz contracted volume,

$$\rho = 2\gamma\rho_0, \tag{54}$$

where $\gamma$ is the Lorentz factor. These two scenarios will approximate the initial or injection point in the phase diagram for each laboratory energy. The trajectory of such injection points in the case of hydrodynamics is known as the Taub or shock adiabat. From the injection point corresponding to a particular bombarding energy, the system will start to evolve since it exists at high pressure and energy density. We approximate the evolution as the path of constant entropy, which we can refer to as quasi-hydrodynamics, since each elementary volume of matter will pass through the same states as would be traced in a hydrodynamic evolution. What we lack in this description is the space-time history.

## 4.3 Phase Transition Dependance on Hadron Spectrum

We show a sample of our results relating to the question of the role played by baryon states beyond the nucleons. These include the $\Delta$ and the hyperons, $\Lambda, \Sigma, \Xi$. Their presence will raise the energy required to heat matter to a given temperature, and under certain circumstances can lead to an abnormal phase transition [8,9,25,26].

In Fig. 7 the only baryons are nucleons interacting through the scalar and vector meson fields. The thermal pions with the two modes discussed earlier are also included. However because of strangeness conservation on the short time scale of the nuclear reaction, thermal kaons do not appear. In Fig.8 the deltas and hyperons and thermal kaons are included as well. In both cases we use $K = 300$ MeV and $m^*_{sat}/m = 0.8$ for the hadronic equation of state, and a bag constant $B^{1/4} = 275$ MeV and $\alpha_s = 0$ for the quark-gluon equation of state. The top panel in each figure shows the phase diagram in the $T - \rho$ plane. The solid lines denote the phase boundaries. The low $T - \rho$ region is the hadronic phase, the region between the two boundaries is the mixed phase, and the high $T - \rho$ region is the quark-gluon phase. The broken lines denote the trajectories that are the injection points accessible to experiment as approximated by the Rankine-Hugoniot shock relation. The dotted line denotes the continuation of the hadronic shock trajectory if no transition to quark-gluon phase were to take place. The squares denote the end points of the mixed phase on the shock trajectory. In the other panels of the figures, the temperature, pressure, density and entropy per baryon are shown on the shock trajectories as functions of the laboratory kinetic energy per projectile nucleon (fixed target) related to the energy per nucleon in the center of mass of the composite system, $\epsilon/\rho$ by,

$$E_{lab} = 2\frac{\epsilon_0}{\rho_0}(\gamma^2 - 1), \quad \gamma = \frac{\epsilon/\rho}{\epsilon_0/\rho_0} \tag{55}$$

These figures show the conditions in which matter is created in a collision, assuming shock dynamics. The figures are qualitatively similar if instead we assume perfect stopping in the overlapping Lorentz contracted volume of the colliding nuclei.

We shall discuss the implications of these figures in the next section. Here our purpose is to note that the baryon resonances play a very important part in defining the phase diagram and especially in determining the energy at which the mixed phase can first be made. The resonances shift the laboratory kinetic energy to higher energy by about a factor two for the present value of $K$ and $B$. This is so approximately independent of these two parameters.

In particular, depending on how strong a role the baryon resonances play, the mixed phase threshold occurs as low as 4 GeV laboratory kinetic energy (fixed target) to as high as 8 GeV, for the bag constant $B^{1/4} = 285$ MeV. For a value of $B^{1/4} = 200$ MeV, the mixed phase begins at 1 GeV to 2 GeV depending on the role of the resonances.

## 4.4 Properties on the Shock Trajectory

In Figs.7 and 8 we showed the properties of matter that are initially produced in a collision assuming shock dynamics and $K = 300$ MeV and $B = 275$ MeV. We discuss the implications of these results. We recall first of all the constancy of the pressure through the mixed phase *on an isotherm*, which has given rise to the suggestion of a plateau in transverse momentum of spectator fragments. As noted in

the introduction, one cannot probe isotherms in collisions, and the consequence of this is clearly seen in the figure. The pressure rises monotonically and with very little change in slope as a function of energy as the phase boundaries are crossed. The difference in pressures that matter would have if it remained in the hadron phase or if it underwent transition to the mixed and quark-gluon phase are very nearly the same, differing by less than ten percent. Nevertheless it is possible that the discontinuity in slope at the ends of the mixed phase, could, in the hydrodynamic flow of the participant region, produce a flattened region in the transverse momentum of spectator fragments. Likewise the entropy signal of a phase transition is very weak. At first these results may seem unexpected, inasmuch as the degrees of freedom are more numerous in the quark-gluon phase, suggesting lower pressure and higher entropy. However for the same reason, for given energy, the temperature of the quark-gluon phase is falls throughout the mixed phase as a function of increasing bombarding energy, which explains the above. In fact, the temperature and the density are the two properties that undergo the greatest discontinuity in behavior as the threshold for the mixed phase is reached. Observables that depend sensitively on these changes in behavior will be the most favorable for detecting the quark-gluon phase. Di-lepton production seems especially favorable. The high temperature of the hadronic phase, if it persists above the transition point to mixed phase, will enhance di-leptons from $\pi^+ - \pi^-$ annihilation. Differences in the photon production may also be a strong signal. These and other results will be the subject of a future publication. (It is interesting to note that the same qualitative features noted above, like the fall of $T$ through the mixed phase were also observed in the calculations of a phase transition of a different type [27].)

A plateau in temperature as a function of energy is frequently mentioned as a qualitative signal of the mixed phase, based on the notion of 'melting' (as of ice in water). The analogy is inaccurate inasmuch as the melting of the hadrons in a sequence of increasingly higher energy nuclear collisions is not a sequence of measurements at constant pressure (as in the heating of a pan of ice in the atmosphere). We have seen instead, as in Fig.8, that the initial conditions, as estimated by the Rankine-Hugoniot shock condition, are characterized by rising pressure and falling temperature as the bombarding energy is increased through the mixed phase. The transverse momentum is usually considered as a measure of the temperature. However the particle momentum of the participant region is determined by both the temperature and the boost provided by the collective flow induced by the high pressure of the expanding matter. The fall of $T$ and rise of $p$, with increasing bombarding energy have opposite effects on the particle transverse momentum and may give rise to a plateau or perhaps a fall in $p_\perp$ through the mixed phase, but not for the reason commonly given and certainly a plateau in temperature cannot be expected.

## 4.5 Dependance on Bag Pressure

For fixed value of the nuclear compression $K = 300$ MeV, and other saturation properties as discussed earlier, including the nucleon effective mass at saturation which is rather well determined, we show in Figs.9 to 12 the phase diagram and properties on the shock trajectory for four values of the bag pressure, $B$ and a fifth one in Fig.8. For reference, $B^{1/4} = 145$ MeV is found to give an overall fit to the baryon mass spectrum that is reasonable [28], while $B^{1/4} = 175$ MeV better reproduces the average of the nucleon and delta mass [29]. On the other hand, from these figures, $B^{1/4} = 250 - 275$ MeV, better reproduces the transition temperature $T \sim 200$ MeV suggested by lattice gauge calculations for the phase transition in baryonless matter. The figures shows an interesting diversity of forms for the phase diagram, depending on $B$. We shall place more emphasis on values of $B$ that give the baryonless phase transition at $T \sim 200$ MeV. It is clear that the value of $B$ that best reproduces the hadron mass spectrum in the MIT bag model gives much too low a transition temperature.

However we draw special attention to Figs.10 and 11 which have a baryonless phase transition at $T \sim 160 - 170$ MeV, which is not so far below the expectations of lattice gauge simulations that these results can be ruled out, especially given the uncertainty in the energy scale of the lattice calculations. The phase boundaries in these cases are of special interest, since the baryonless transition is in the range of lattice QCD, but falls rapidly in $T$ as the density increases, so that the mixed phase appears as low as $T = 115$ MeV, $\rho = 4.7\rho_0$ and $E_{lab} = 2.5$ GeV.

For each $K$ there is a maximum $B$ above which the behavior is unphysical in the sense that below a critical baryon density $\rho_c$ no transition to the quark phase occurs, and above this density the system alternates between the two phases as the temperature is increased. This however is an artifact of the two-model approach to the phase transition. On an isotherm in the $p - \mu$ plane the isotherms for the two phases intersect more than once. It is more plausible that once the critical conditions for transition from hadronic to quark matter are exceeded, the system remains in the second phase for all higher conditions. Such a situation is shown in Fig.13 in the $T - \rho$ plane.

## 4.6 Dependance on Gluon Exchange

Corrections to the simple equation of state of free quarks and gluons from gluon exchange are uncertain, but we include a sample calculation in which lowest order perturbation interaction is taken into account with $\alpha_s = 0.2$ in Fig.14. Comparison with Fig.12 shows that interactions raise the laboratory energy at which the mixed phase is reached by about fifty percent.

## 4.7 Dependance on Nuclear Compression $K$

We compare similar results to those discussed in the last section for other values of the nuclear compression modulus, $K = 220$ and 250 MeV, in Figs.15 16. These can be compared with the results for $K = 300$ MeV and the corresponding $B$ in Figs.11 and 12 respectively. Very little sensitivity to $K$ is evident in these results and this is true for $K$ within the range $\sim 220 - 350$ MeV except at the larger $B$ as discussed in an earlier section.

The relative insensitivity to the uncertainties in the nuclear equation of state as represented by $K$ (and $m^\star$ within its range of uncertainty), can be understood from Figs.1, 2 where we see that the thermal energy is much bigger than the energy differences due to uncertainties in $K$ or $m^\star$.

## 4.8 Dependance on Pion Spectrum in Medium

We saw in an earlier section that the pion spectrum is strongly altered in the medium. Indeed there are two important excitations having the pion quantum numbers, which at low $k$ are pion-like and delta-like, and which interchange their character at higher $k$, above $k_0$. In all of the calculations discussed above we have included both modes, using for the Landau parameter, $g'(m_\pi/g_\Delta)^2 = 0.7$. The thermal pions will be especially important in high temperature matter and this is born by comparing Fig.17 for which the free pion dispersion is used and Fig.8 where both pion excitations are included according to section 2.3. We see that the mixed phase is shifted to higher energy, since it corresponds to temperatures in the range $T = 155 - 175$.

Besides the Landau parameter, $g'(m_\pi/g_\Delta)^2 = 0.7$, we also tried a smaller value, 0.5, but the change was negligible, suggesting that the most important part of the medium correction is the low to moderate density, high $k$ region corresponding to the large isobar component where the rescattering effect is smaller.

# 5 Summary

We have studied a two part model of the transition between hadron and quark-gluon phases of matter in the energy domain of nuclear stopping. The hadronic phase is described by nuclear field theory including among the baryons, the nucleons deltas and hyperons, interacting through the scalar and vector meson fields. Pions and kaons were included as thermal populations and in the case of pions their spectrum in the medium due to $\Delta - N^{-1}$ (and the corresponding antiparticle) excitations was calculated. The quark-gluon plasma phase was described by the equation of state for massless $u$ and $d$ quarks and gluons and massive $s$ quarks, including interactions in lowest order perturbation theory. For this two part model we calculated the phase diagram and the shock trajectory through it as an example of the injection point of the collision dynamics. We stressed that the dynamics of the collision does not

permit the experimental exploration of the entire phase diagram. Matter properties at the injection point as a function of bombarding energy were calculated through hadron to mixed to quark-gluon phase. Most remarkable was the fall in temperature through the mixed phase with increasing bombarding energy. Di-leptons should provide a means of detecting the fall as compared to a continued rise in $T$ in a pure hadronic phase.

A strong dependance on the hadronic spectrum was found to be registered in the phase diagram and the properties of matter on the shock trajectory. A significant dependance on the modification of the pion spectrum from its free to in medium one was also found. The first is a hundred percent increase in the threshold energy of the mixed phase, and the second a forty percent increase.

The hadronic equation of state is prescribed at all densities in nuclear field theory by the properties at saturation, since these define the coupling constants except for those of the higher baryon states (deltas and hyperons). The greatest uncertainty concerns the compression modulus. The nucleon effective mass at saturation has the potential of effecting the high density equation of state even more, but we believe that it is pinned down to a narrow range. The effect of both, within their range of uncertainty, on the finite temperature equation of state that is probed in collisions is largely masked by the thermal energy, and little sensitivity of the phase diagram or the properties of matter on the shock trajectory is found.

Beside the hadronic spectrum and the pion medium effects, the phase diagram is most strongly effected by the bag constant and the QCD coupling constant.

In these calculations the highest density at which matter in the hadronic phase can be produced is 3.7 to 7.7 times nuclear density, depending on the factors discussed above. The corresponding temperature for the finite baryon density matter is $T \sim 150 - 180$ MeV, for those bag constants that yield a baryonless phase transition at $T \sim 200$ MeV. To the extent that the baryonless phase transition at $T \sim 150$ MeV is compatible with lattice QCD, then the threshold of the mixed phase could occur at Laboratory kinetic energy as low as 2.5 GeV with $T \sim 100$ MeV, but otherwise could occur as high as 9 GeV. Both are compatible with the uncertainties in the plasma equation of state as inferred from the baryonless transition temperature, and depend very little on uncertainties with which the nuclear equation of state can be defined in terms of conventional nuclear properties at saturation, because of the dominance of the thermal energy.

Although the application here is to laboratory energies corresponding to nuclear stopping, the general nature of the results apply also to situations of partial transparency. In this latter case, the relation between the laboratory energy and the energy density of the created matter are not simply related, and depend on the degree of transparency. Our energy scales should therefore be replaced by the corresponding energy density, which would have then to be related by a plausible model to the beam energy. In other words, in the general situation, the energy scale on our figures should be considered as multiplied by an unknown scaling factor.

**Acknowledgements**: I thank L. P. Csernai, J. I. Kapusta and M. Gyulassy

for helpful discussions. This work was supported by the Director, Office of Energy Research, Office of High Energy and Nuclear Physics, Division of Nuclear Physics, of the U.S. Department of Energy under Contract DE-AC03-76SF00098.

# References

[1] B. Sevitsky, Nucl. Phys. **A461** (1987) 71c.

[2] F. Karsch, Nucl. Phys. **A461** (1987) 305c.

[3] L. P. Csernai, in *Hadronic Matter in Collision*, ed. P. Carruthers and D. Strottman, World Scientific Press, 1986.

[4] D. H. Rischke, B. L. Friman, H. Stocker and W. Greiner, J. Phys. G, **14** (1988) 191.

[5] K. S. Lee, M. J. Rhoades-Brown and U. Heinz, Phys. Rev. C **37** (1988) 1452.

[6] L. P. Csernai, "The Nuclear Equation of State", University of Bergen Scientific report 195/1988;
L. P. Csernai, M. Gong and D. D. Strottman, "Pion Distribution from the Fluid Dynamical Model of Ultra-relativistic Heavy Ion Collisions", University of Bergen Scientific report 196/1988.

[7] P.-G. Reinhard, M. Rufa, J. Maruhn, W. Greiner and J. Friedrich, Z. Phys. **A323** (1986) 13.

[8] S. I. A. Garpman, N. K. Glendenning and Y. J. Karant, Nuc. Phys. **A322** (1979) 382.

[9] N. K. Glendenning, Phys. Lett. **185B** (1987) 275;
N. K. Glendenning, Nucl. Phys. **A469** (1987) 600.

[10] N. K. Glendenning, Phys. Lett. **114B** (1982) 392;
N. K. Glendenning, Astrophys. J. **293** (1985) 470;
N. K. Glendenning, Z. Phys. **A 326** (1987) 57;
N. K. Glendenning, Z. Phys. A, **327** (1987) 295.

[11] E. Beth, and G. E. Uhlenbeck, Physica **4** (1937) 915;
S. Z. Belenkij, Nucl. Phys. **2** (1956) 259;
R. Dashen, S. K. Ma and H. J. Bernstein, Phys. Rev. **187** (1969) 345.

[12] N. K. Glendenning, Phys. Rev. C **37** (1988) 2733.

[13] M. M. Sharma, W. T. A. Borghols, S. Brandenberg, S. Crona, A. van der Woude and M. N. Harakeh, Phys. Rev. C **38** (1988) 2562.

[14] G. Peilert, H. Stocker, W. Greiner, A. Rosenhauer, A. Bohnet and J. Aichelin, (UFTP preprint 214/1988), submitted to Phys. Rev. C.

[15] C. H. Johnson, D. J. Horen and C. Mahaux, Phys. Rev. C **36** (1987) 2252.

[16] A. B. Migdal, Rev. Mod. Phys. **50** (1978) 107.

[17] B. Banerjee, N. K. Glendenning and M. Gyulassy, Nuc. Phys. **A361** (1981) 326.

[18] G. Baym, Nuclear Physics with Heavy Ions and Mesons, Vol. 2, Les Houches Sesion XXX, ed. R. Balian, M. Rho and G. Ripka (North Holland, Amsterdam, 1978)p. 745.

[19] B.Friedman, V. R. Pandharipande and Q. N. Usmani, Nucl. Phys. **A372** (1981) 483.

[20] R. Bauer, J. Speth, V. Klempt, P. Ring, E. Werner, and T. Yamazaki, Nucl. Phys. **A209** (1973) 535.

[21] L. H. Xia, C. M. Ko, L. Xiong and J. Q. Wu, Nucl. Phys. bf A485 (1988) 721.

[22] S. A. Chin, Phys. Lett. **78B** (1978) 552.

[23] J. I. Kapusta, Nucl. Phys. **B148** (1979) 461.

[24] O. K. Kalashnikov and V. V. Klimov, Phys. Lett. **88B** (1979) 328.

[25] N. K. Glendenning, *Phase Transitions in Nuclear Matter* in 7th High Energy Heavy Ion Study, 1984, ed. R. Bock, H. H. Gutbrod and R. Stock (GSI report-85-10).

[26] J. Theis, G. Grabner , G. Buchwald, J. Maruhn, W. Greiner, H. Stocker, J. Polonyi, Phys. Rev. D **28** (1983) 2286;
T. Nakai and S. Takagi, Prog. Theor. Phys. **71** (1984) 1118.

[27] N. K. Glendenning, Phys. Lett. **144B** (1984) 158.

[28] T. DeGrand, R. L. Jaffe, K. Johnson, and J. Riska, Phys. Rev. **D12** (1975) 2060.

[29] J. Cleymans, R. V. Gavai and E. Suhonen, Phys. Rep. **130** (1986) 217.

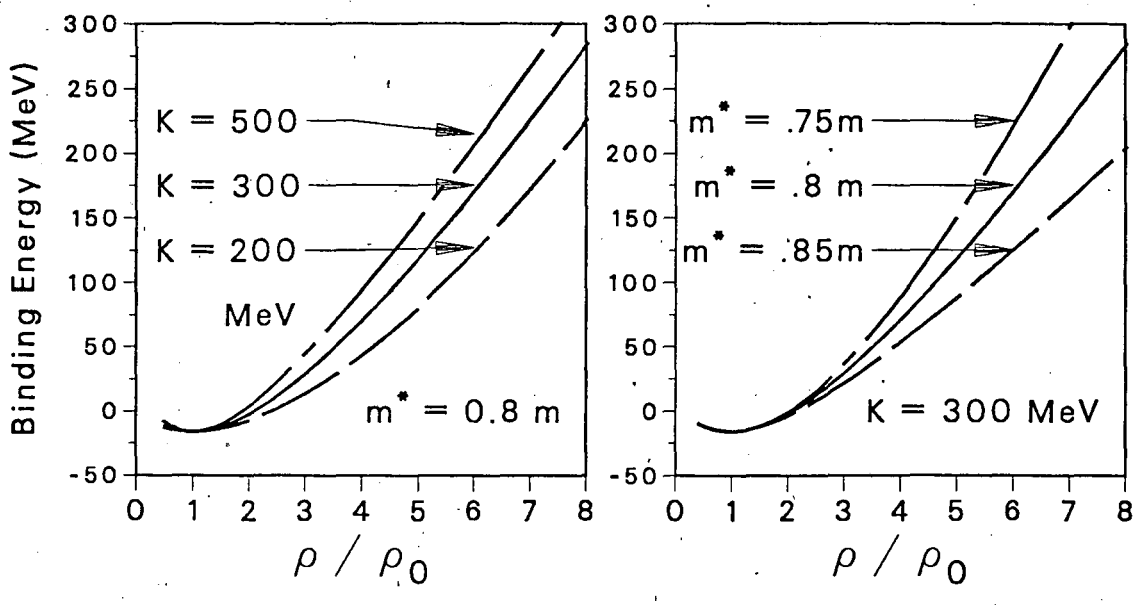


-- XBL 891-198 --

Figure 1: Equation of state for several $m^*$ and $K$ within the relevant density range.

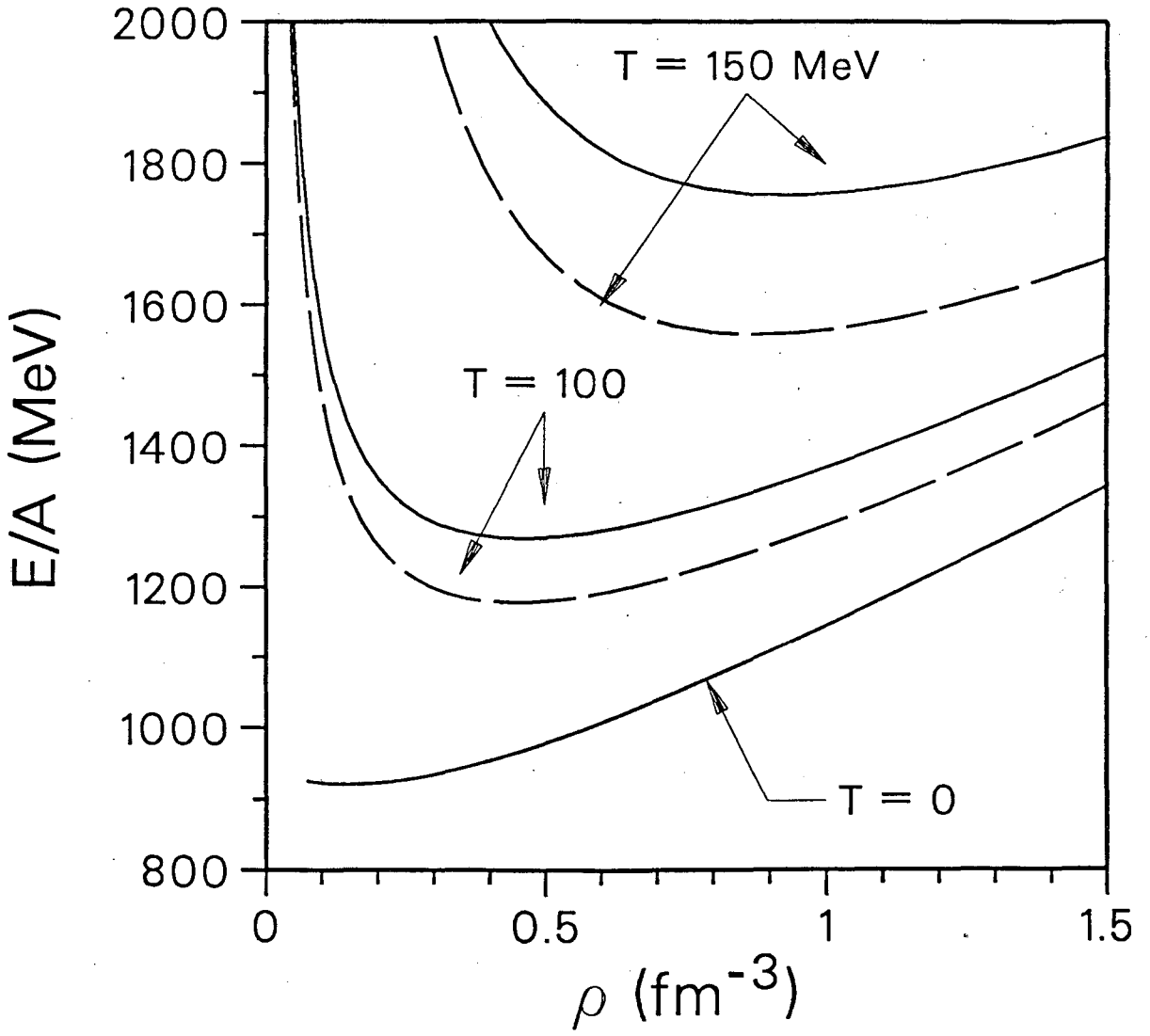


-- XBL 891-199 --

Figure 2: Energy per baryon on several isotherms. Solid line includes all hadron states in Table 1, while dashed line includes only the nucleons and pions.

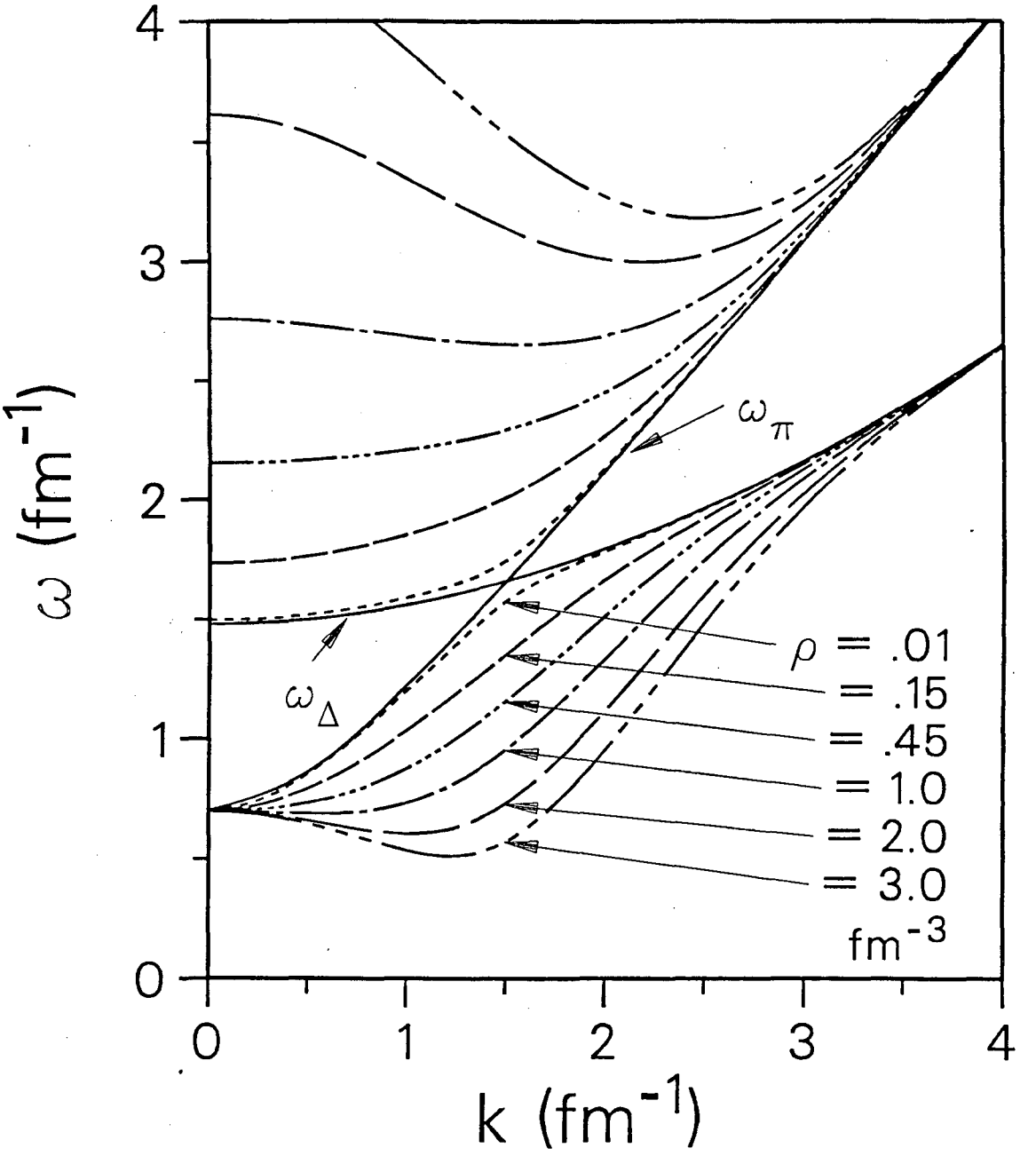


-- XBL 891-200 --

Figure 3: The free pion and isobar ($\Delta - N^{-1}$) spectra are shown by $\omega_\pi$ and $\omega_\Delta$ respectively and the pion spectrum in nuclear matter at various baryon densities are shown by the other curves.

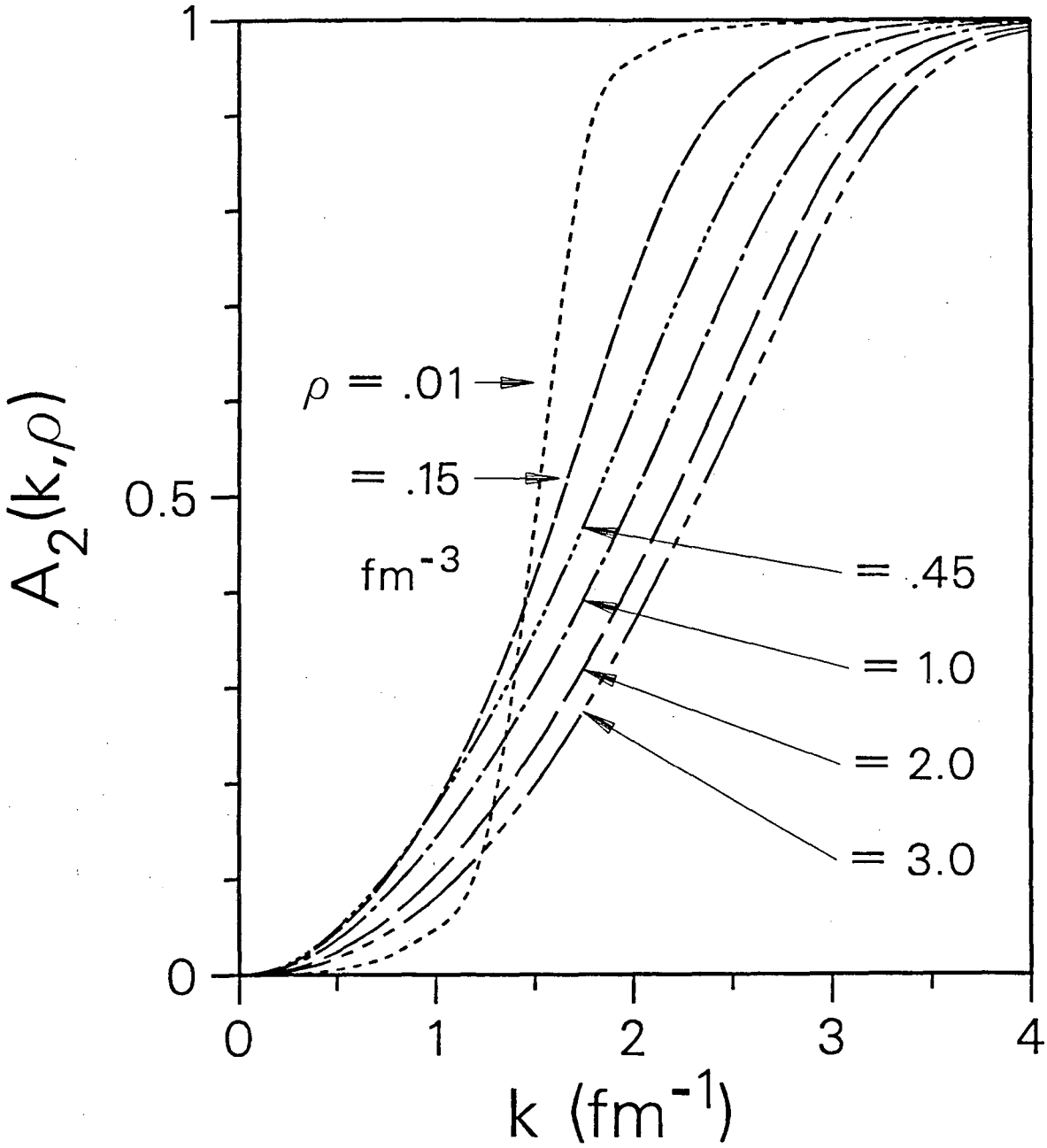


-- XBL 891-201 --

Figure 4: Weight for the pion-like component in the mode 2 for several nuclear densities $\rho$. The other amplitude is $A_1 = 1 - A_2$.

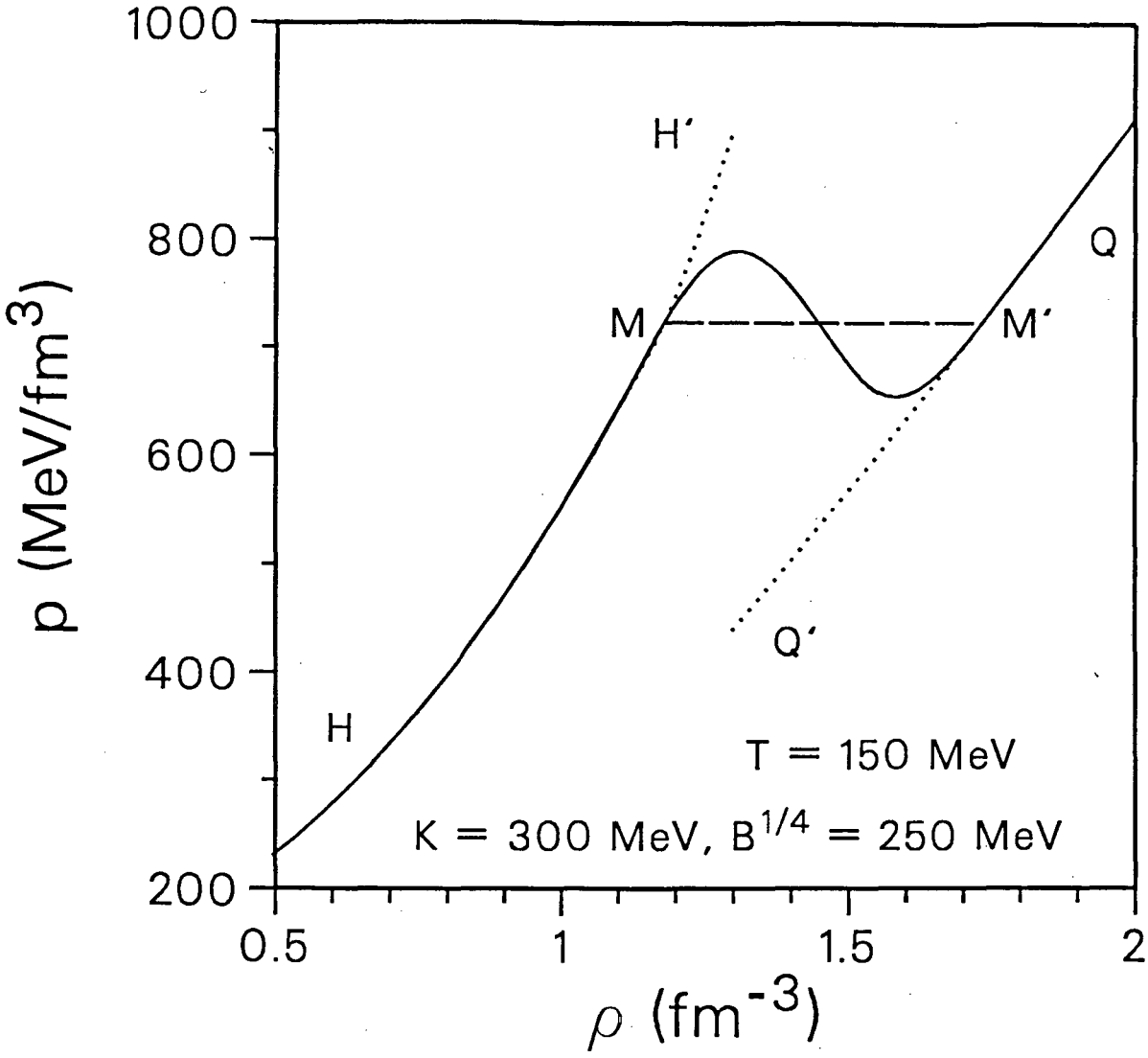


-- XBL 891-202 --

Figure 5: Pressure as a function of baryon density on an isotherm with $T = 150 MeV$. The curve HM is the hadron phase, MM' the physical mixed phase and MQ is the quark phase. The solid curve between MM' is a schematic of a complete theory (lattice QCD) in the region of mixed phase. The dotted lines MH' and Q'M' are the extensions of the hadron and quark phases.

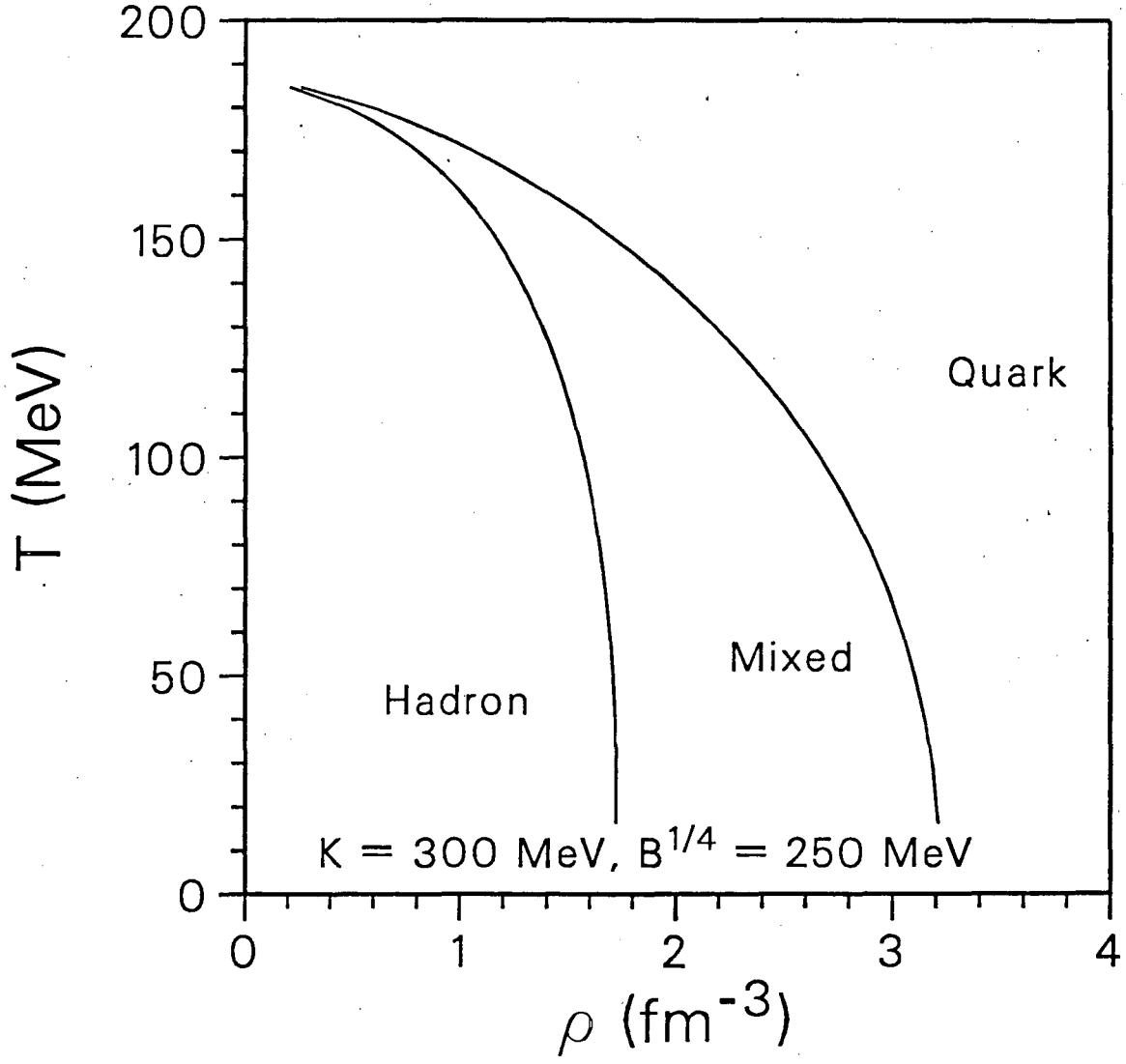


-- XBL 891-203 --

Figure 6: Phase diagram showing hadron, mixed and quark-gluon phase, for nuclear compression $K = 300$ MeV and bag pressure $B^{1/4} = 250$ MeV.

Figure 7: In top panel phase boundaries (solid lines) and the shock trajectories (broken). Other panels show properties of matter along the shock trajectory. Hadronic phase includes nucleons, mean field mesons and thermal pions in medium. $B^{1/4} = 275$ MeV, $K = 300$ MeV

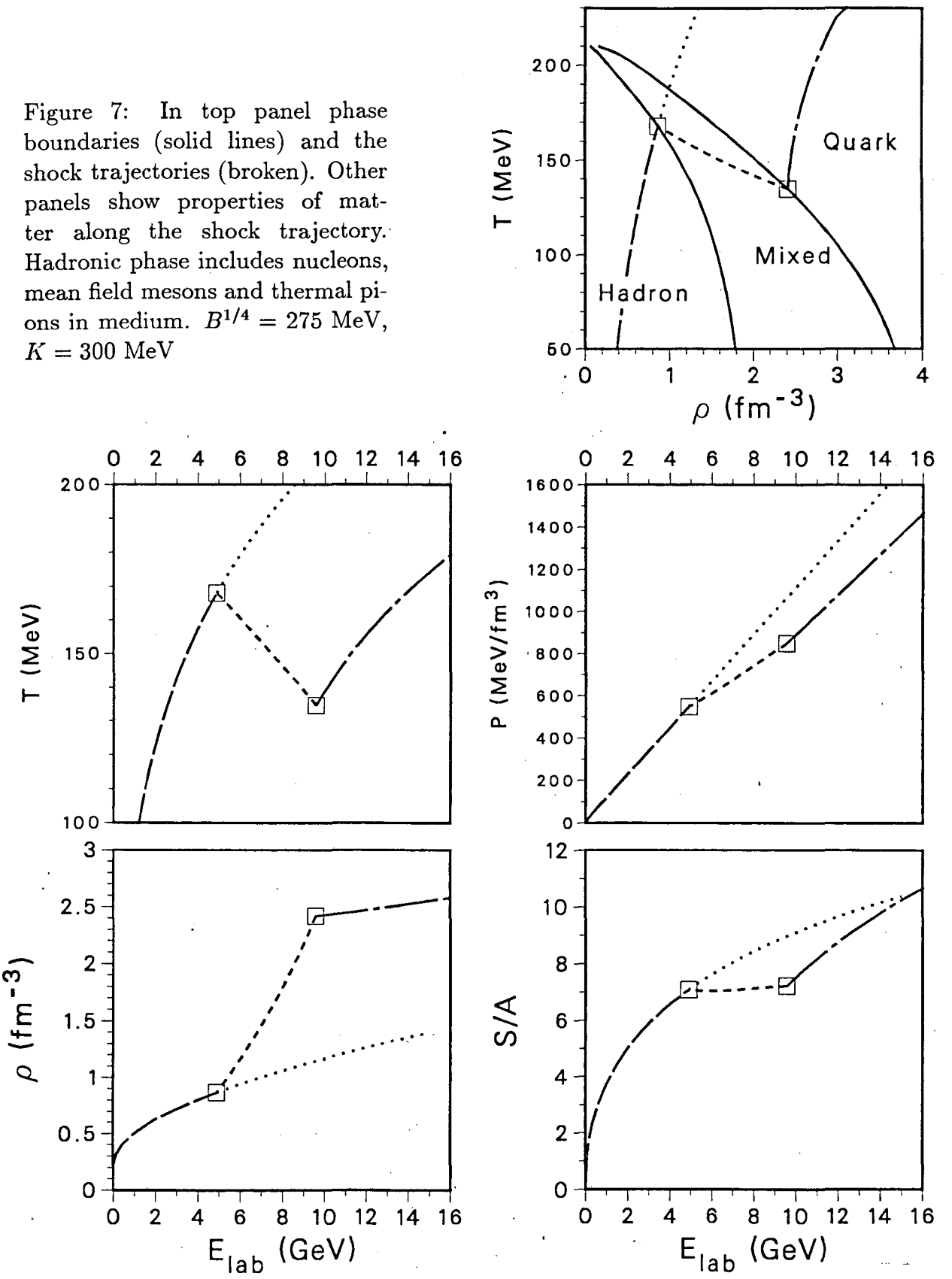


-- XBL 891-204 --

Figure 8: In top panel phase boundaries (solid lines) and the shock trajectories (broken). Other panels show properties of matter along the shock trajectory. Hadronic phase includes nucleons, deltas, hyperons, mean field mesons and thermal pions (with medium effects) and kaons. $B^{1/4} = 275$ MeV, $K = 300$ MeV

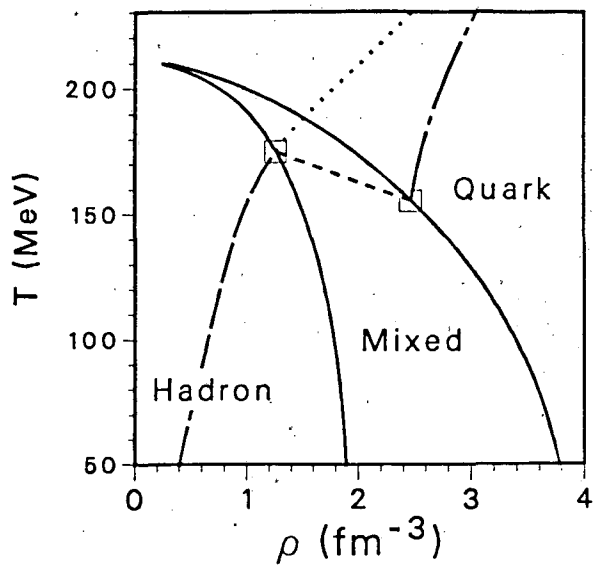


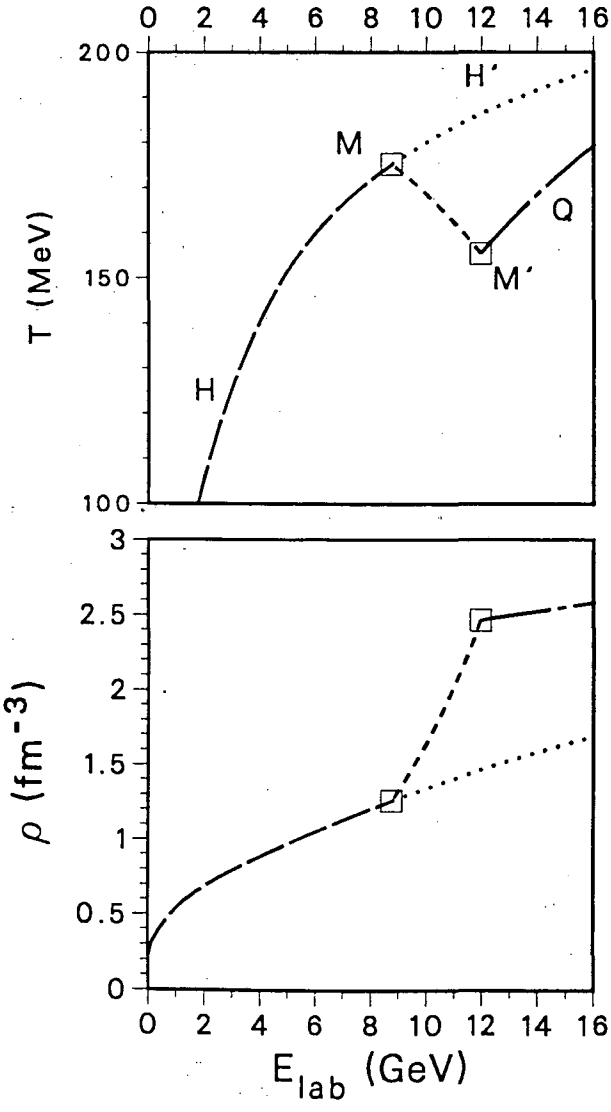


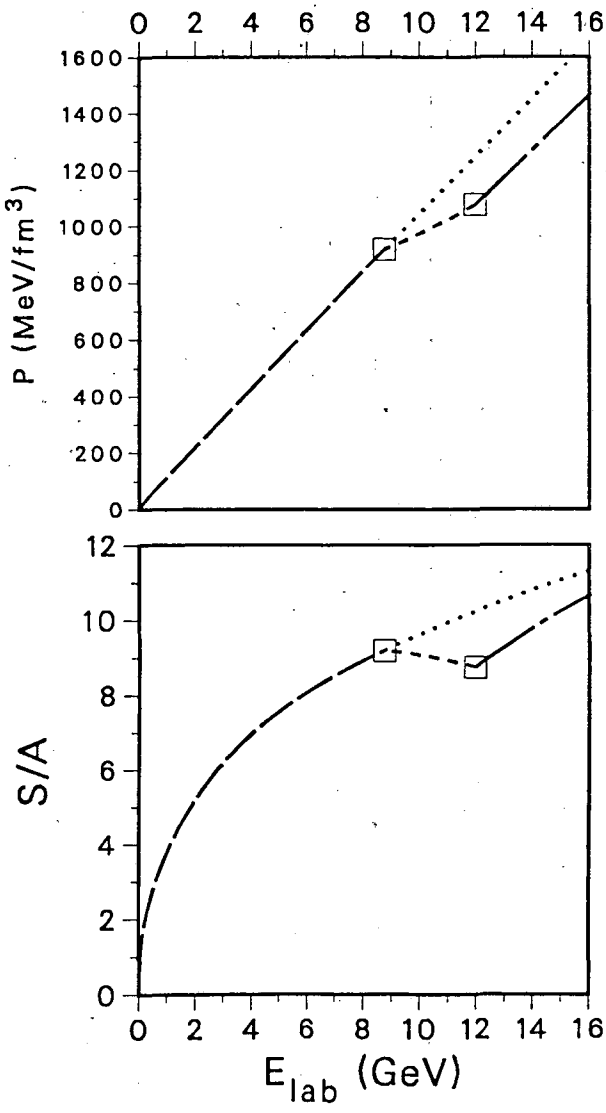


-- XBL 891-207 --

Figure 9: Same as Fig. 8 but $B^{1/4} = 175$.

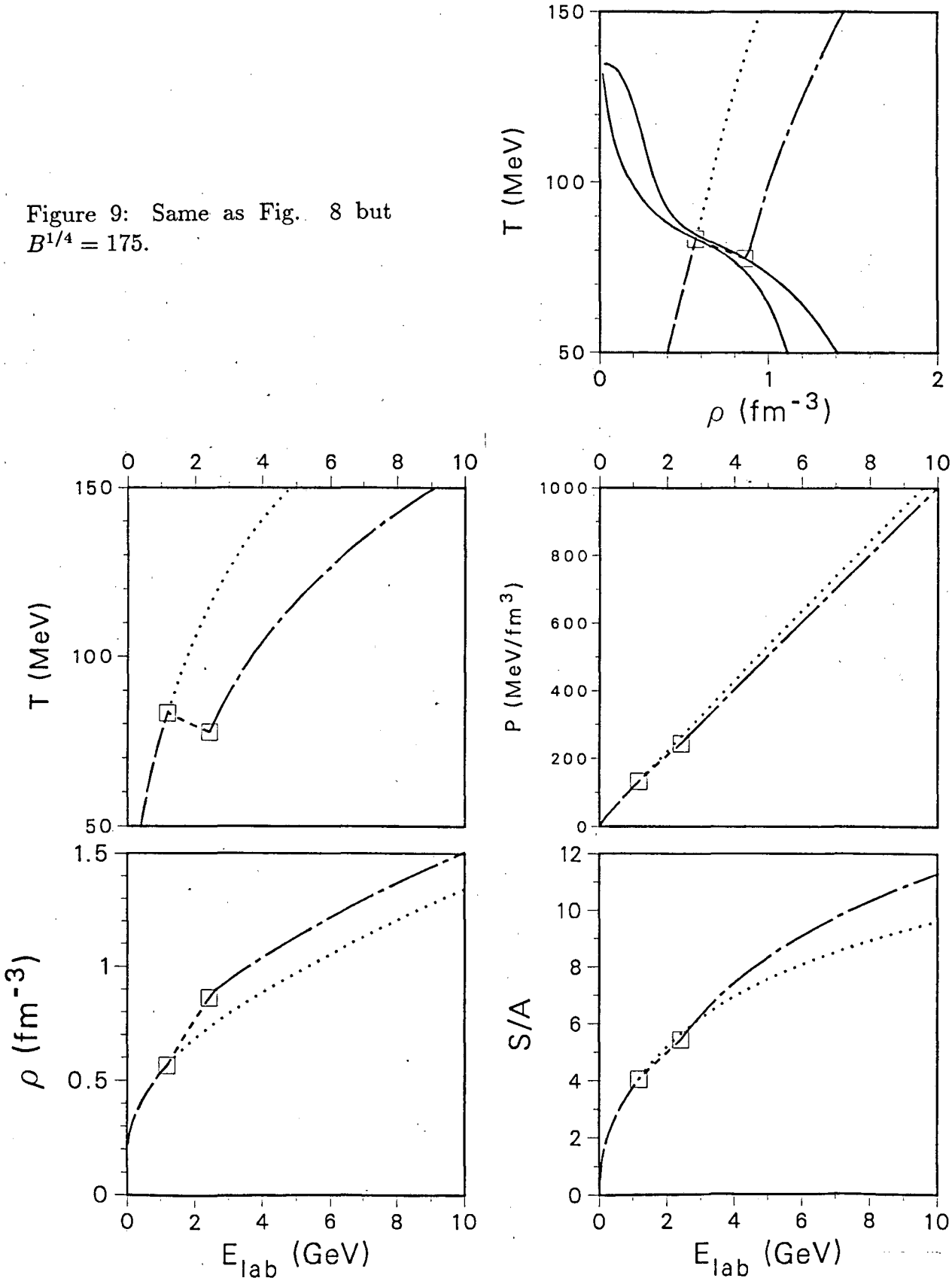


-- XBL 891-205 --

Figure 10: Same as Fig. 8 but $B^{1/4} = 200$.

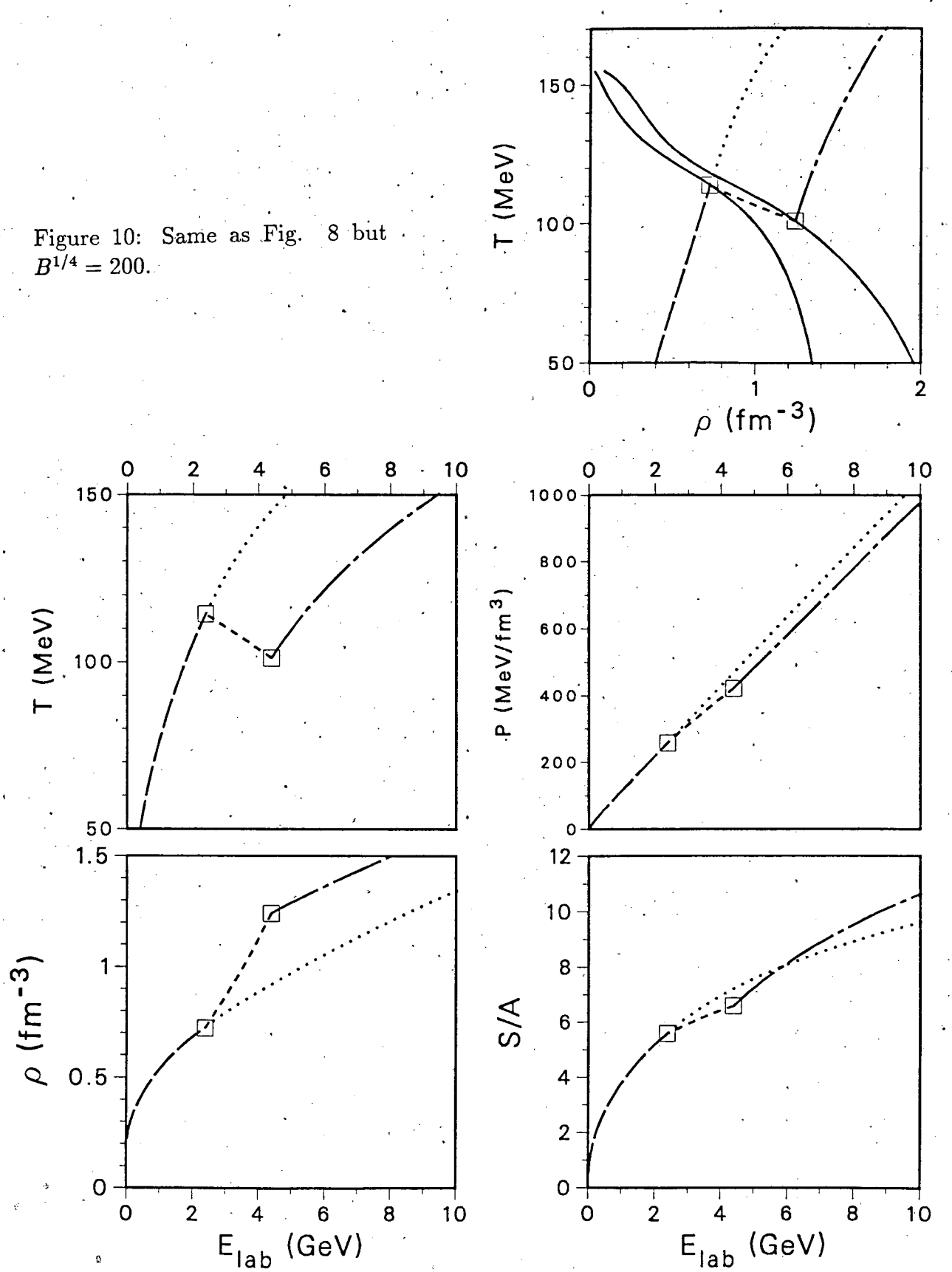


-- XBL 891-206 --

Figure 11: Same as Fig. 8 but $B^{1/4} = 225$.

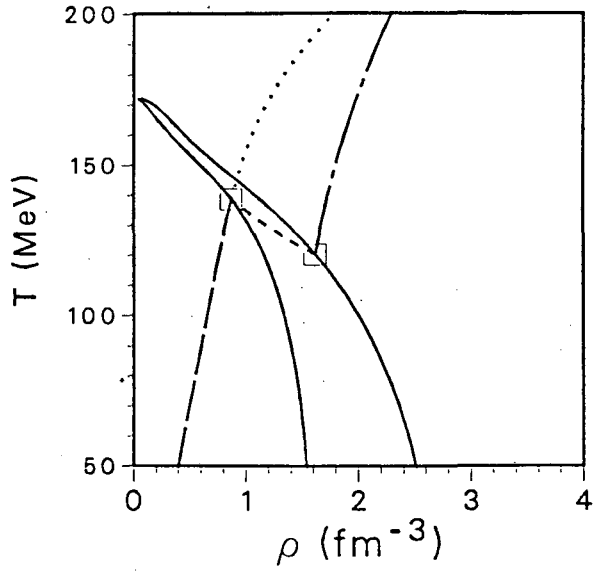


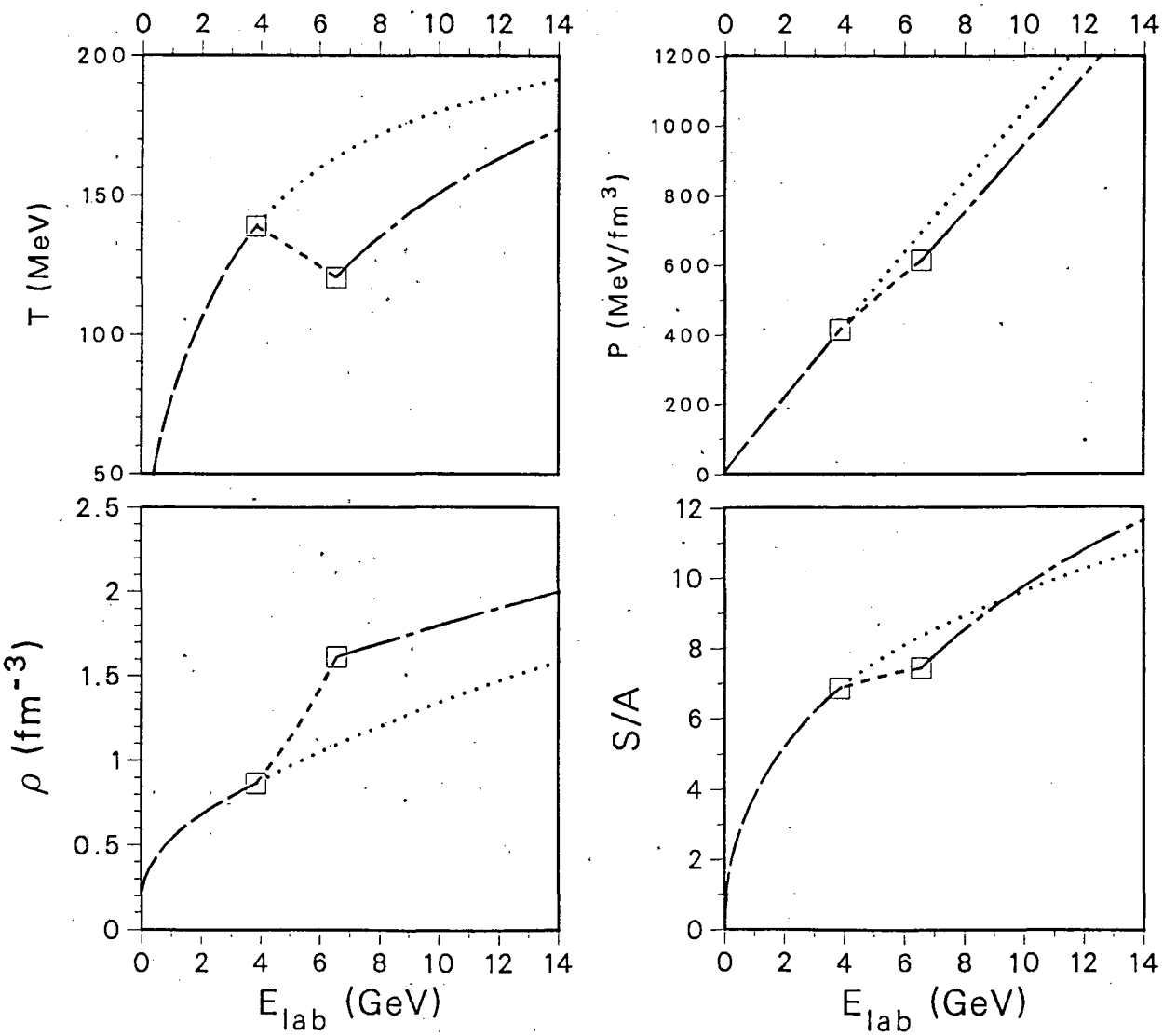


-- XBL 891-208 --

Figure 12: Same as Fig. 8 but $B^{1/4} = 250$.

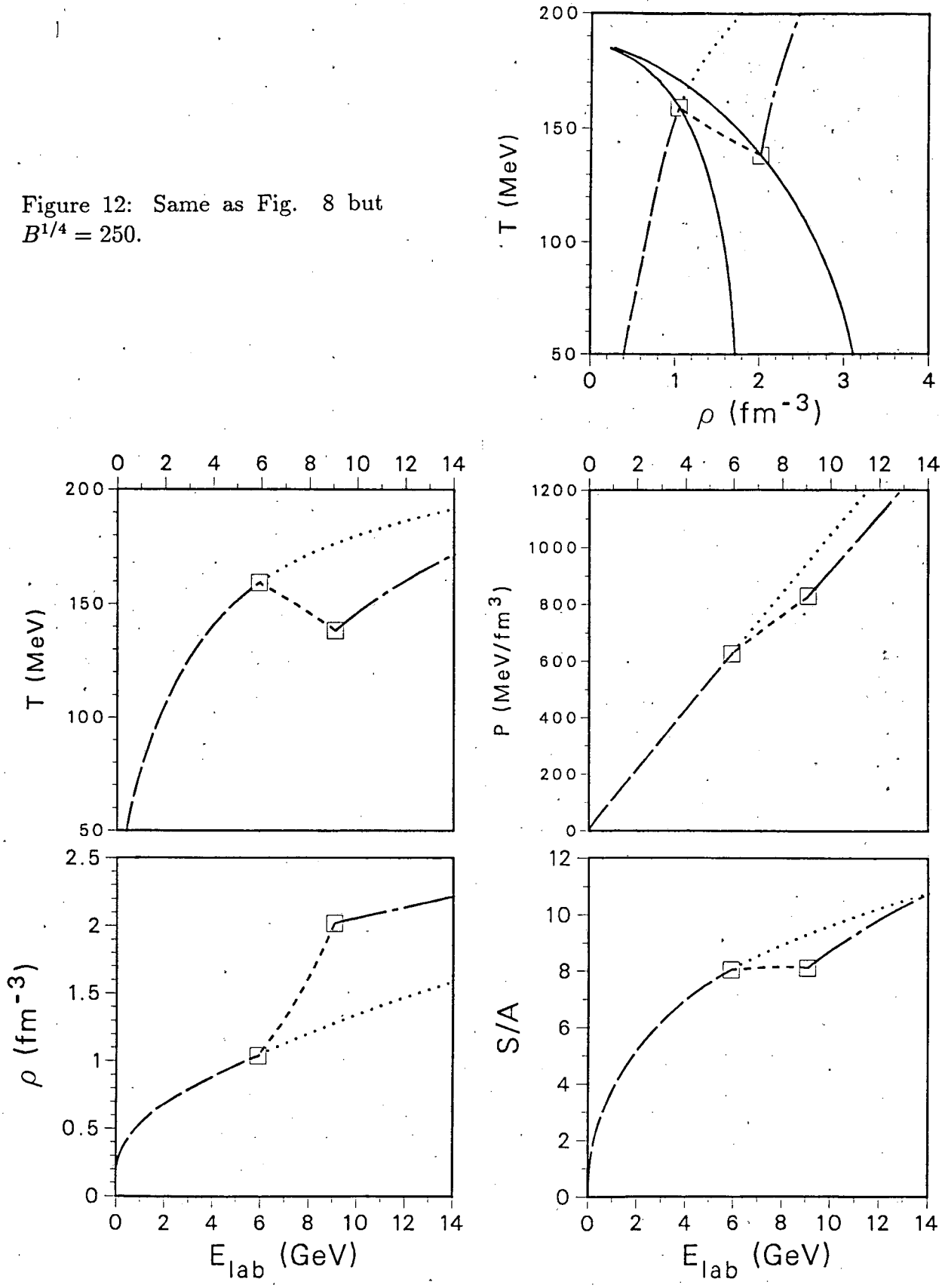


-- XBL 891-209 --

Figure 13: Same as Fig. 8 but $B^{1/4} = 300$ MeV.

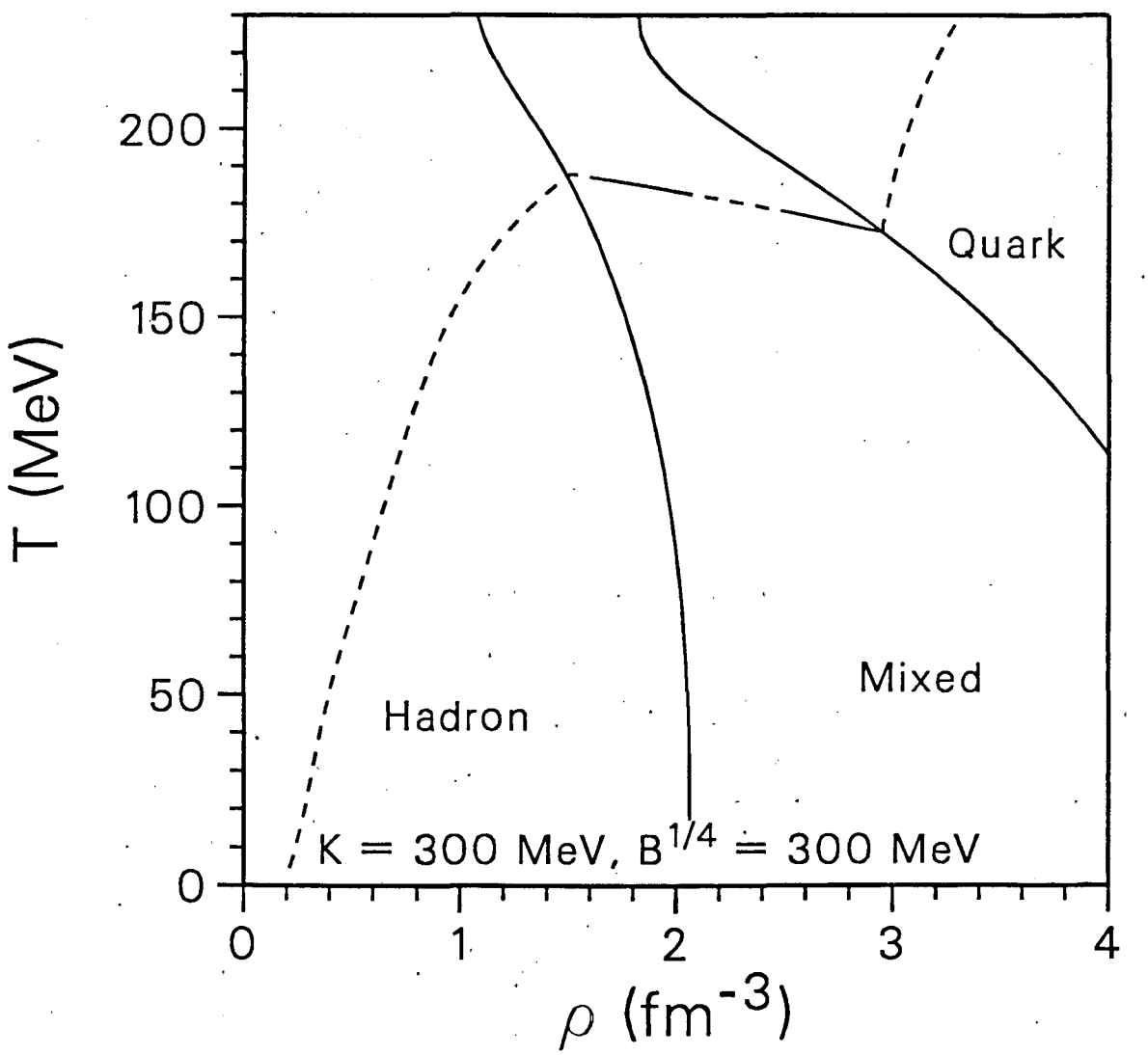


-- XBL 891-210 --

Figure 14: Showing effect of interactions in the quark-gluon phase for $\alpha_s = 0.2$. Compare with Fig.12. In both cases, $B^{1/4} = 250$ MeV and $K = 300$ MeV.

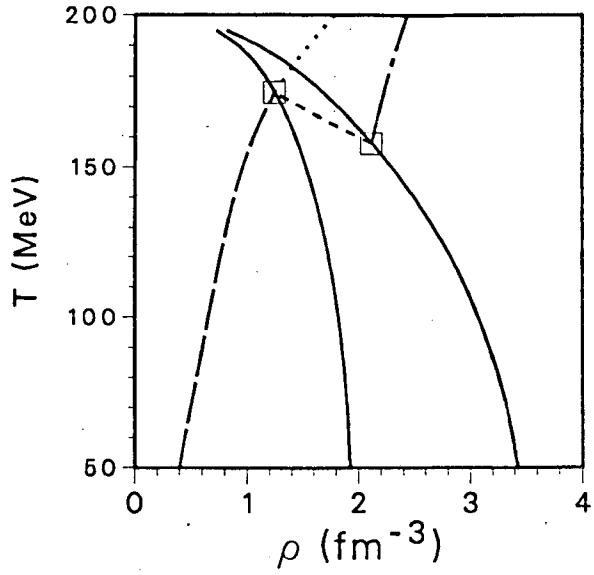


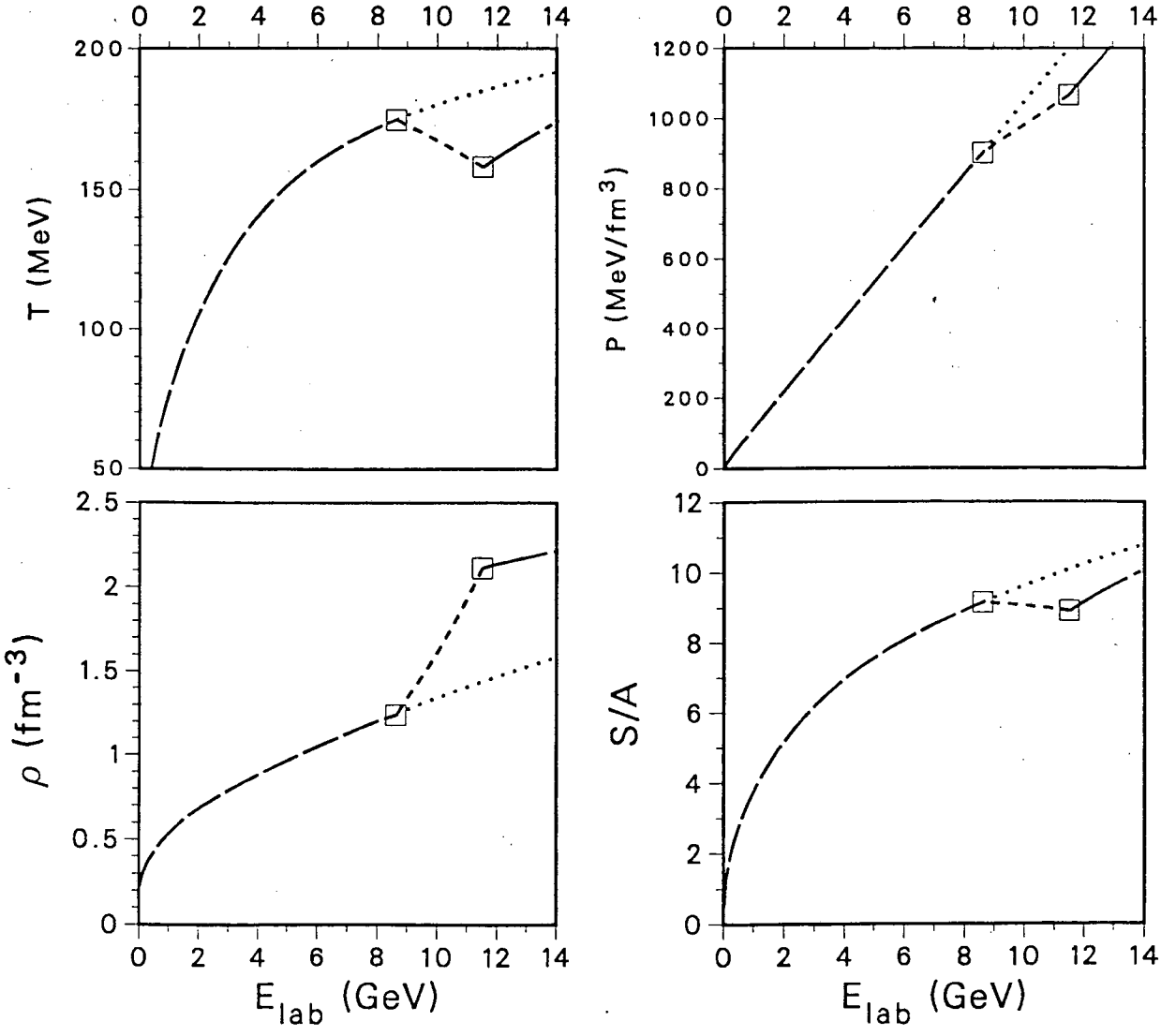


-- XBL 891-212 --

Figure 15: Same as Fig. 11 but $K = 220$.

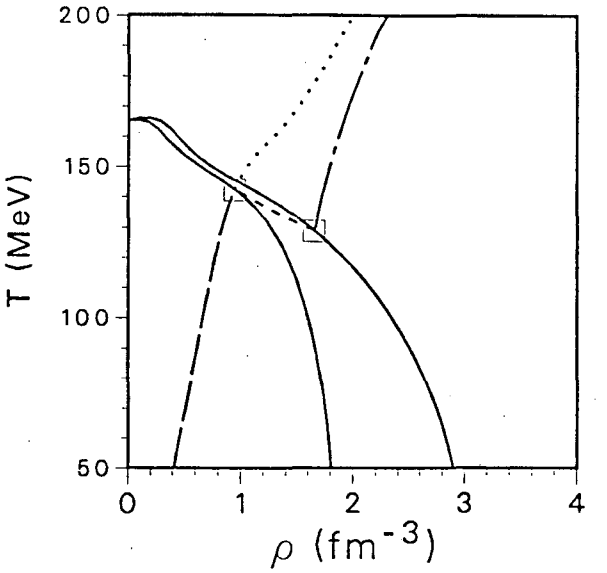


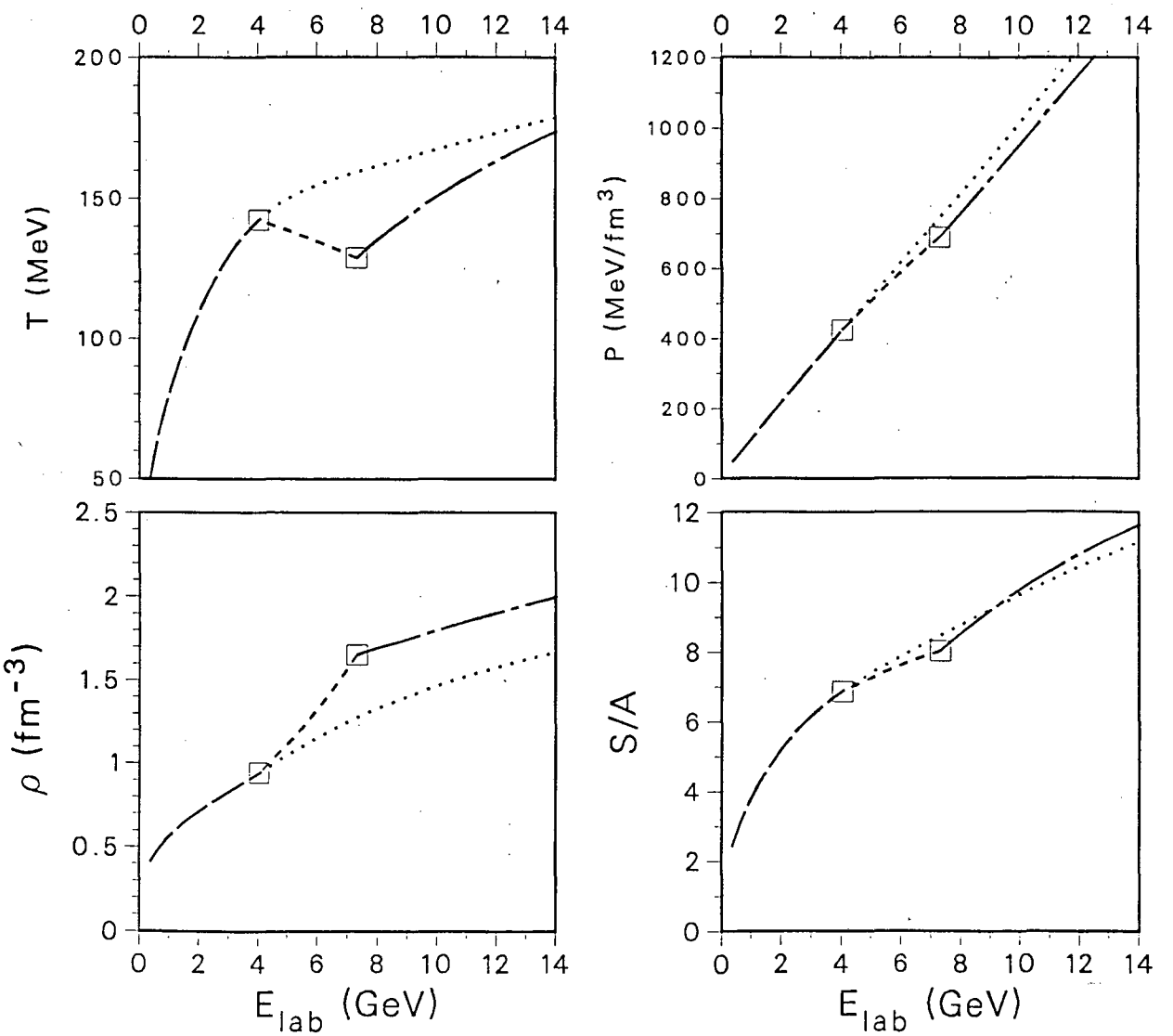


-- XBL 891-213 --

Figure 16: Same as Fig. 12 but $K = 250$.

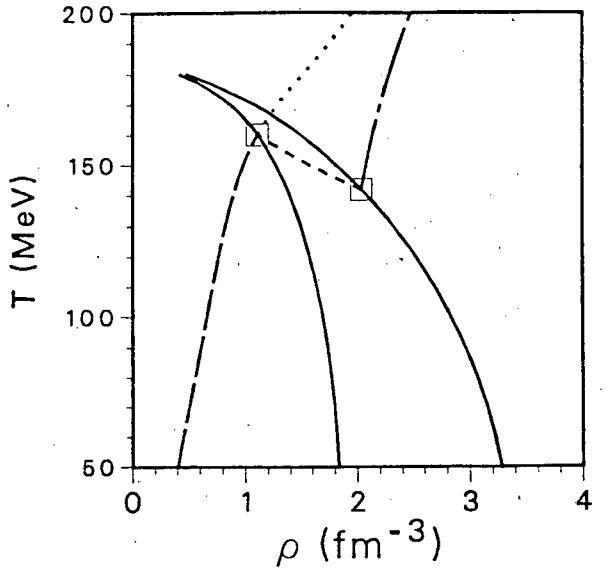


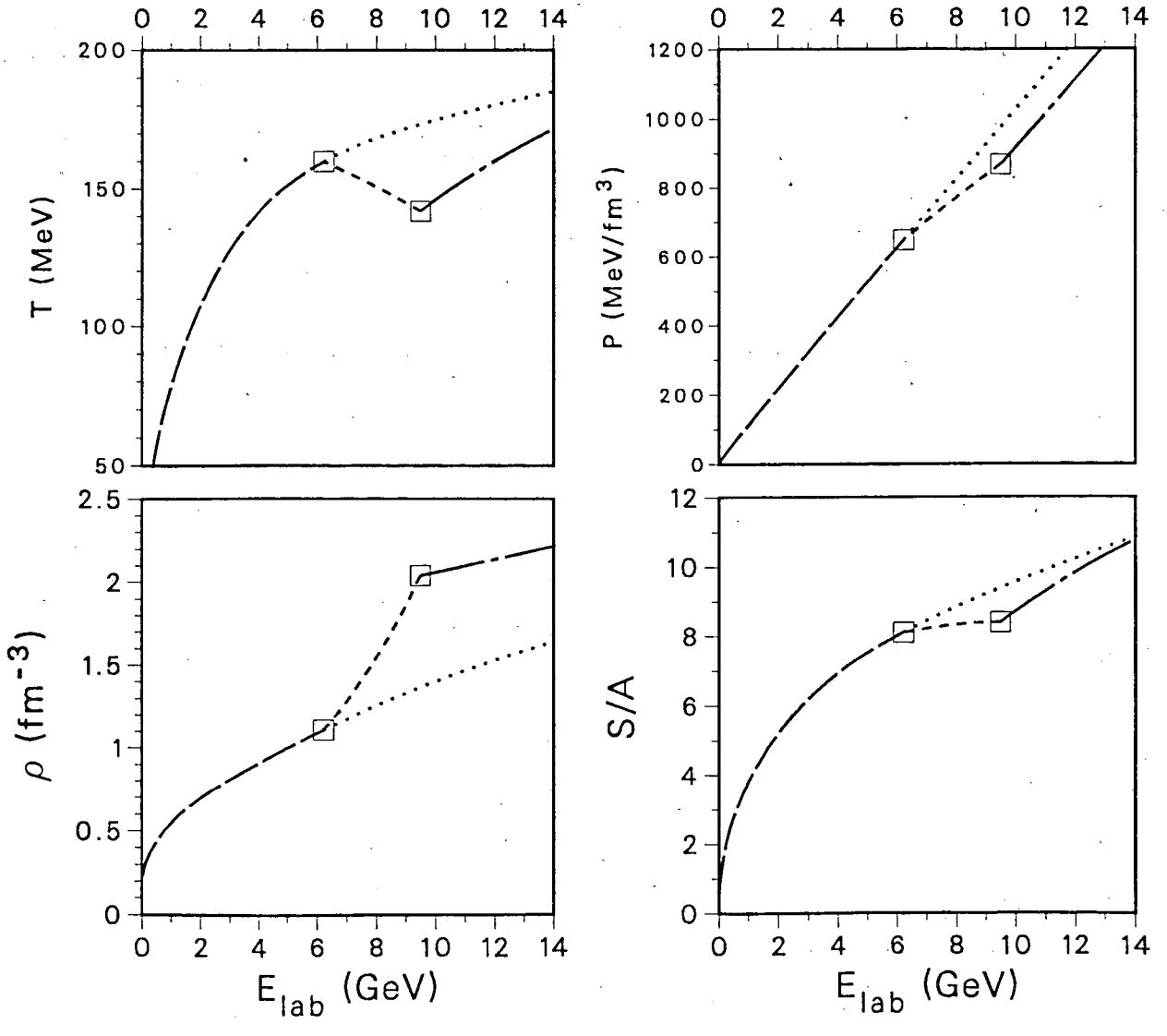


-- XBL 891-214 --

Figure 17: Same as Fig. 8 but instead of in medium pions, the free pion spectrum is used.

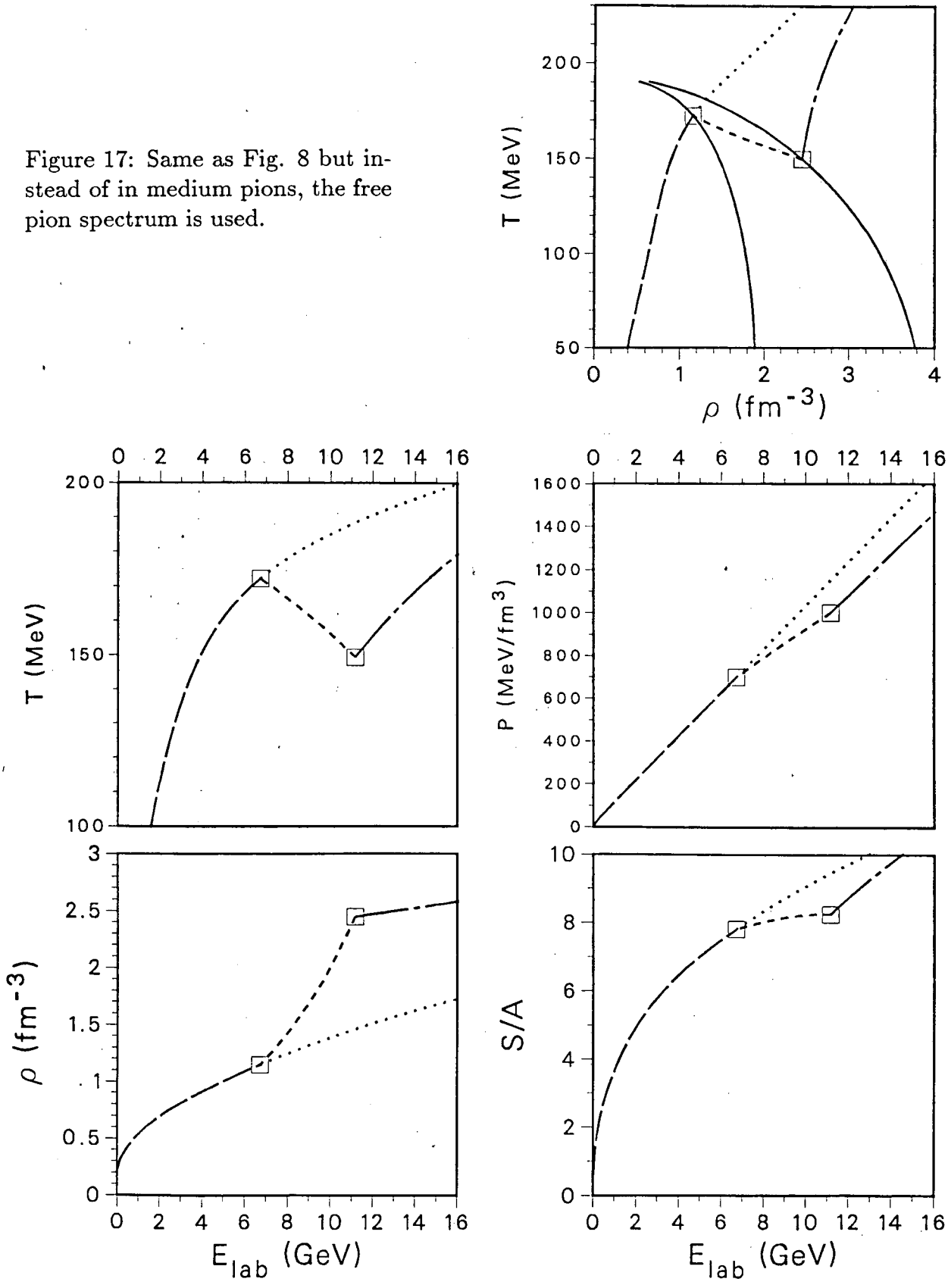


-- XBL 891-215 --

LAWRENCE BERKELEY LABORATORY
TECHNICAL INFORMATION DEPARTMENT
1 CYCLOTRON ROAD
BERKELEY, CALIFORNIA 94720